

UNIVERSITY OF CALIFORNIA

Los Angeles

Investigation of Physical Activity Monitors and their Relationship to Traditional Physiological Measures during Human Exercise

A thesis submitted in partial satisfaction of the requirements for

the degree Master of Science

in Physiological Science

by

Marlon Lacson Abrazado



2012

Abstract of the Thesis

Investigation of Physical Activity Monitors and their Relationship to Traditional
Physiological Measures during Human Exercise

by

Marlon Lacson Abrazado

Masters of Science in Physiological Science

University of California, Los Angeles, 2012

Professor Alan Garfinkel, Co-Chair

Professor Christopher B. Cooper, Co-Chair

Purpose: Accelerometry data from 2 physical activity monitors (PAM) paired with 3 physiological measures (heart rate, oxygen uptake, and energy expenditure) across 3 exercise modes (constant treadmill load, stepping, and incremental treadmill exercise).

Methods: 10 males performed 9 intensities each of steady-state treadmill and stepping exercise with wrist- and ankle-mounted PAMs. Last 2 minutes of each exercise was defined as steady-state, where energy expenditure (EE), derived by indirect calorimetry, and vector magnitude units (VMU), derived from accelerometer vectors, were averaged. Seven combinations of PAM configuration were compared. 2-factor ANOVA determined the effect of speed, grade, and their interaction for treadmill exercise, and the effect of step height, step rate, and their interaction for stepping exercise. 10 different, equally healthy subjects performed 3 incremental treadmill exercise tests with a chest-mounted

PAM. Slopes from $HR/\dot{V}O_2$ and HR/VMU were compared, with repeatability assessed by intraclass correlation coefficients (ICC).

Results: Mean EE (Kcal/min) for all steady-state exercises ranged between 3 and 18 kcal/min 2-factor ANOVA revealed no effect of grade on all PAM configurations during treadmill exercise. ICC for $HR/\dot{V}O_2$ slopes = 0.80 ICC for HR/VMU slopes = 0.31

Discussion: PAM output was not influenced by grade for any configuration, which can be problematic for predicting EE. Slopes and intercepts of $HR/\dot{V}O_2$ was deemed more repeatable across 3 incremental exercise tests than HR/VMU.

Committee

The thesis of Marlon Lacson Abrazado is approved.

Thomas W. Storer

Victor R. Edgerton

William J. Kaiser

Alan Garfinkel, Committee Co-chair

Christopher B. Cooper, Committee Co-chair

University of California, Los Angeles

2012

Dedication

To say Dr. Christopher Cooper has been a wonderful mentor would be an understatement. I thank him tremendously for all the years I have been graciously mentored by him and have been received valuable insight and advice for both my career and personal life. He has been incredibly patient, accepting and graciously generous for funding my graduate education, and for that I am eternally grateful.

Special thanks to Dr. Thomas Storer, who has contributed greatly by navigating me through academia and providing me with quality insight into career development. I am appreciative for the lessons learned in precision, scientifically rigorous testing, analysis and data interpretation.

I only wish to have colleagues as intellectually enriching and loyal, while remaining life-long friends as both Drs. Cooper and Storer have been together.

Many thanks as well to Dr. Brett Dolezal, who has been served as a role model for me in the past few years. His sense of humor and ambition has stimulated a positive working environment.

Furthermore, many thanks to the supporting staff (Amy Chen, Milan Patel, John Wheeler, Patsy Rivera, and John Dermand) for their emotional support and encouragement. Additionally, many thanks to the study participants for their extra time and effort in the laboratory; this research would not have existed without them.

I'd also like to thank my wife Berlinda and son Christian. This journey together for the past several years has been one of our lives' most challenging tests, and I am glad to have had them by my side.

Table of Contents

Abstract of the Thesis	ii
Committee.....	iv
Dedication	iv
Table of Contents.....	vii
List of Figures.....	x
List of Tables.....	xii
List of Abbreviations	xiii
Acknowledgements	xiv
Introduction	1
Study 1. Interrelationship between Accelerometer Location, Energy Expenditure and Exercise Mode	4
Subjects.....	4
Methods.....	5
Instrumentation.....	6
Statistical Analysis	7

Results	11
Study 2. Interrelationship between Accelerometry, Heart Rate and Energy Expenditure	14
Subjects	14
Methods	15
Exercise Protocol.....	15
Instrumentation	16
Statistical Analysis	18
Independent Variables.....	18
Derivation of Additional Variables: Work and Energy Expenditure	18
Heart Rate and Respiratory Rate Reliability	19
Validity of Integrated Activity Measures	19
Proof of Concept for Cardiocaloric Index	19
Reliability of CI and CCI.....	20
Results	21
Discussion.....	25

Appendix A: Figures	36
Appendix B: Tables	74
References	89

List of Figures

- Figure 1: PAM model X6-2 and axis orientation. (Gulf Data Concepts, LLC. Waveland, MS).
- Figure 2: PAM Locations on extremities.
- Figure 3: Variable organization in matrix format.
- Figure 4: Example of time-synchronization between oxygen uptake and activity counts for one subject.
- Figure 5: Stackplot of one subject's oxygen uptake during defined steady-state for all treadmill intensities (s1-s9).
- Figure 6: Stackplot of one subject's oxygen uptake during defined steady-state for all stepping intensities (s1-s9).
- Figure 7: Integrated physical activity (ΣA) for all limbs plotted against energy expenditure for all treadmill intensities.
- Figure 8: Integrated physical activity (ΣA) for all limbs plotted against energy expenditure for all stepping intensities.
- Figure 9: Stackplot of r^2 for seven different PAM configurations for treadmill exercise. LA=left arm, RA=right arm, BA=both arms, BL=both legs, AL=all limbs.
- Figure 10: Stackplot of r^2 for seven different PAM configurations for stepping exercise. LA=left arm, RA=right arm, BA=both arms, BL=both legs, AL=all limbs.
- Figure 11: Distribution of simulated F-like statistics for treadmill exercise. (red line = calculated F-statistic. black vertical lines demarcate the 95% confidence interval).
- Figure 12: Distribution of simulated F-like statistics for stepping exercise. (red line = calculated F-statistic. black vertical lines demarcate the 95% confidence interval).
- Figure 13: Confidence intervals for two-way ANOVA parameters for energy expenditure during treadmill exercise.
- Figure 14: Confidence intervals for two-way ANOVA parameters for energy expenditure during stepping exercise.
- Figure 15: Confidence intervals for two-way ANOVA parameters for PAM activity counts (Left Arm) during treadmill exercise.
- Figure 16: Confidence intervals for two-way ANOVA parameters for PAM activity counts (Left Arm) during stepping exercise.
- Figure 17: Confidence intervals for two-way ANOVA parameters for PAM activity counts (Right Leg) during treadmill exercise.
- Figure 18: Confidence intervals for two-way ANOVA parameters for PAM activity counts (Right Leg) during stepping exercise.

- Figure 19: Estimated treatment means plot for both speed and grade on energy expenditure (left panel) and PAM activity counts for left arm (right panel) for treadmill exercise.
- Figure 20: Estimated treatment means plot for both speed and grade on energy expenditure (left panel) and PAM activity counts for left arm (right panel) for stepping exercise.
- Figure 21: Estimated treatment means plot for both speed and grade on PAM activity counts for right leg for treadmill exercise.
- Figure 22: Estimated treatment means plot for both speed and grade on PAM activity counts for right leg (right panel) for stepping exercise.
- Figure 23: Confidence intervals for two-way ANOVA parameters for PAM activity counts (All Limbs) during treadmill exercise.
- Figure 24: Confidence intervals for two-way ANOVA parameters for PAM activity counts (All Limbs) during stepping exercise.
- Figure 25. Paired heart rates for all exercise data.
- Figure 26. Bland-Altman for paired heart rates for all exercise data. Top and bottom horizontal lines signify ± 1.96 standard deviations.
- Figure 27. Paired breathing frequencies for all exercise data.
- Figure 28. Bland-Altman for paired breathing frequencies for all exercise data. Top and bottom horizontal lines signify ± 1.96 standard deviations
- Figure 29. Linear increase in workrate over time for WFI Run protocol for each subject across 3 trials.
- Figure 30. Linear increase in $\dot{V}O_2$ over workrate for each subject across 3 trials.
- Figure 31. Linear increase in VMU over workrate for each subject across 3 trials.
- Figure 32. Linear increase in VMU against EE for each subject across 3 trials.
- Figure 33. Linear increase in heart Rate against workrate for each subject across 3 trials.
- Figure 34. Chronotropic indices for each subject across 3 trials.
- Figure 35. Stackplot with error bars for chronotropic indices.
- Figure 36. Cardiocaloric indices for each subject across 3 trials.
- Figure 37. Stackplot with error bars for cardiocaloric indices.
- Figure 38. Linear regression for chronotropic index slope against cardiocaloric index slope.

List of Tables

Table 1. Treadmill Matrix

Table 2. Stepping Matrix

Table 3. Subject Characteristics for Steady-State Exercise

Table 4: Median Percentage of Variability (r^2) in Measured Energy Expenditure Explained by PAM

Table 5. Median Percentage of Variability (r^2) in Measured Energy Expenditure Explained by PAM

Table 6. 2-factor ANOVA on PAM activity from Different Configurations for Treadmill Exercise

Table 7. 2-factor ANOVA on PAM activity from Different Configurations for Stepping Exercise

Table 8: Subject Characteristics for Incremental Exercise

Table 9. Speed and Grade Settings for WFI Run Protocol

Table 10. Pearson R Correlations for HR Validity

Table 11. Single-factor ANOVA for Chronotropic Index Slopes Grouped by Trials

Table 12. Single-factor ANOVA for Chronotropic Index Slopes Grouped by Subjects

Table 13. Single-factor ANOVA for Cardiocaloric Index Slopes Grouped by Trials

Table 14. Single-factor ANOVA for Cardiocaloric Index Slopes Grouped by Subjects

Table 15: Statistical Parameter Summary for Incremental Treadmill Exercise

List of Abbreviations

PAM	Physical Activity Monitor
ΣA_{LL}	Sum of Activity measured at Left Leg
ΣA_{RL}	Sum of Activity measured at Right Leg
ΣA_{BL}	Sum of Activity measured at Both Legs
ΣA_{LA}	Sum of Activity measured at Left Arm
ΣA_{RA}	Sum of Activity measured at Right Arm
ΣA_{BA}	Sum of Activity measured at Both Arms
$\Sigma A_{BL,BA}$	Sum of Activity measured at Both Legs and Both Arms
FA	Effect of Speed in Treadmill or Step Height in Stepping Exercise
FB	Effect of Grade in Treadmill or Step Rate in Stepping Exercise
FAB	Effect of Interaction (Speed and Grade or Step Height and Rate)
\dot{W}	Workrate
$\dot{V}O_2$	Rate of Oxygen Uptake
$\dot{V}CO_2$	Rate of Carbon Dioxide Output
EE	Energy Expenditure (derived from Oxygen Uptake)
HR.bh	Heart Rate measured by Zephyr Bioharness 2
HR.ox	Heart Rate measured by Oxycon Pro 12-lead ECG
VMU	Activity in Vector Magnitude Units measured by Zephyr Bioharness 2
CI	Chronotropic Index (Linear correlation between HR.ox and $\dot{V}O_2$)
CCI	Cardiocaloric Index (Linear correlation between HR.bh and VMU)

Acknowledgements

The experimental work in this thesis was supported in part by the US Department of Homeland Security Science and Technology Directorate.

Introduction

Self-reported questionnaires for recall of physical activity (PA) have been problematic in that the volume of exercise has typically been overestimated by the user¹. The utilization of physical activity monitors (PAMs) allows for objective measurement of PA, avoiding subjective biases such as subject recall. For example, PAMs have been useful in quantifying volumes of exercise, as a function of duration multiplied by intensity of free-living activities.²⁻⁶

The basic construct of PAMs is an accelerometer chip (piezoelectric, micromechanical springs, or capacitance) and a small mainboard equipped with a lithium battery and memory chip (Figure 1). The minimal size requirements of the hardware allow PAMs to be worn unobtrusively on the body without impeding the activity under study. In recent years, PAMs have undergone extensive development, ranging from simple uni-axial accelerometers to multi-sensor physiological monitors equipped with tri-axial accelerometers and instrumentation for concurrently measuring physiological variables such as heart rate, respiratory rate, or galvanic skin temperature.

When worn on the body, PAM accelerometers are designed to detect and record acceleration and deceleration at user-specified sampling frequencies. Furthermore, these signals can then be recorded continuously with high-frequency sampling for monitoring free-living activity or specific bouts of exercise. Additionally, multi-axial accelerometers have the advantage of measuring motion along multiple axes, which can contribute to the overall profile of movements performed during physical activity.

Combined with physiological sensors, these accelerometers can then supplement accelerometer profiles with physiological data to further differentiate intensities of physical activity⁷. PAMs have been evaluated at various body sites, including the extremities, waist, and chest. However, the optimal PAM location is not known.

Several studies have attempted to correlate energy expenditure (EE) with PAM data across a variety of activities such as walking, running, vigorous sports, and activities of daily living⁸⁻¹³. These studies have attempted to predict EE by 1) classifying the activities performed by intensity (e.g. light, moderate, or vigorous) and 2) summing the associated predicted levels of caloric expenditure.

For instance, PAMs have been shown to be moderately accurate for predicting EE for repetitive locomotor, self-paced activities such as walking, running and climbing steps, but less accurate for non-repetitive movements^{8,13,14}. In studies conducted by Crouter et al, EE derived by indirect calorimetry was compared with uni-axial accelerometry data measured across various activities of daily living^{8,14,15}. In regression analysis, remarkable linearity was demonstrated between EE and tri-axial accelerometry during sedentary and walking activities¹⁶. However, ambulatory exercises utilized in these experiments were primarily flat-ground, steady-state exercises, as EE predictions from uni-axial PAMs were not sensitive to grade changes in treadmill exercise¹⁷. Hence, the question remains whether EE prediction for exercises that involve a vertical component (e.g. graded treadmill or stepping exercise) is improved with the usage of tri-axial accelerometers. By implementing new instrumentation in the laboratory, conventional physiological variables such as heart rate (HR), oxygen uptake ($\dot{V}O_2$), and breathing

rate can be measured at the same time as accelerometry. It may be possible that accelerometry measures obtained by PAMs may be used in describing physiological measures such as energy expenditure or cardiovascular response to exercise.

Typically, PAMs have been designed to attempt to only predict energy expenditure by quantifying total physical activity, but limited research, to our knowledge, is available on fusing physiological data from multi-sensor PAMs with accelerometry data for acute bouts of exercise.

Moreover, recent research by Plasqui et al. measured heart rate separately with activity counts, a raw unit of measure of accelerometer output, from tri-axial accelerometers as a new unit of measure during free-living activity¹⁸. Tönis et al. also measured heart rate and accelerometry separately during steady-state walking tests to predict $\dot{V}O_2max$. In this experiment, linear regression was used to relate steady-state heart rate and accelerometry over two different walking speeds as an indication of exercise intensity¹⁹. However, two issues arise from this methodology: 1.) the relationship of these two parameters was dependent on manual time-synchronization of both the heart rate monitor and accelerometer and 2.) this analysis was limited to walking exercise only.

Our aim in this study was to examine the relationships between the outputs from two physical activity monitors and three traditional physiological measures (HR, $\dot{V}O_2$, and EE). These physiological measures and PAM activity were compared across three specific modes of exercise (constant treadmill load, stepping, and incremental treadmill exercise).

The work of this thesis is divided into two studies. Study 1 describes the influence of accelerometer location on summated PAM vectors and examines the effect of speed or grade and step height or step rate on PAM activity and directly measured EE during steady-state treadmill and stepping exercise, respectively. Study 2 compares the interrelationship between HR with $\dot{V}O_2$ and PAM activity during incremental treadmill exercise.

Study 1. Interrelationship between Accelerometer Location, Energy Expenditure and Exercise Mode

In the first part of this paper, a PAM device was utilized that outputs raw accelerometer signals with the goal of predicting human energy expenditure in response to changes in speed and grade during walking and running. Our approach was to apply multiple tri-axial accelerometers during performance of a range of exercise intensities using steady-state treadmill and stepping exercises and to compare PAM output with actual energy expenditure directly measured via oxygen uptake.

Subjects

Ten healthy subjects (8 men, 2 women) from the University of California, Los Angeles and surrounding neighborhoods volunteered to participate. The subject characteristics are shown in Table 3. Most subjects were physically active according to American College of Sports Medicine criteria performing 30 minutes or more of moderate intensity exercise 5 days or more per week. Subjects were required to refrain from caffeine for 4

hours prior to testing and from intense physical activity for 24 hours. Subjects were also instructed to consume a light meal prior to testing. The study protocol was reviewed and approved by UCLA Institutional Review Board prior to study initiation. Each participant gave written informed consent and procedures were reviewed in detail prior to participation.

Methods

Exercise Protocol

Subjects performed matrices of treadmill and stepping exercises consisting of nine different intensities. The different intensities were achieved using combinations of speed and grade for the treadmill or step height and step rate for the stepping exercise. The speed and grade combinations for treadmill exercise were 2.5, 4.0, and 5.5 mph and 0, 2.5, and 5% grade (Table 1). The nine stepping intensities were developed from step heights of (6, 10, and 20 inches) and step rates of 12, 24, and 30 steps per minute (Table 2). All treadmill exercise was performed on a previously calibrated treadmill ergometer (Trackmaster TMX425. Trackmaster, Newton, KS). Stepping was carried out on adjustable steps designed for the purposes of this study.

Subjects were instructed to maintain the specified speed and grade settings and step height and step rate for six minutes with the goal of achieving or approximating steady-state oxygen uptake at each of the nine intensities.

Subjects were instructed to report to the laboratory at approximately the same time of day for each testing session. After each treadmill and stepping intensity was performed, each subject was monitored until their heart rate had returned to baseline (resting) levels prior to continuing.

Instrumentation

Physical Activity Monitors

Four PAM devices (USB Accelerometer X16-2. Gulf Coast Data Concepts, Waveland, MS), provided by UCLA Wireless Health Institute, were affixed on subjects' right and left ankles and wrists (Figure 2), with each oriented so that the y-axis was vertical with the subject in an upright posture. The PAMs continuously recorded acceleration vectors at a frequency of 160 Hz from each of the x, y, and z axes. The data was written directly into *.csv files, with each row corresponding to 1/160th of a second, and 3 columns corresponding to x, y, and z axes. After 100,000 rows were filled with recorded data, each PAM created a new *.csv file for recording. All csv files were automatically stored on a 1GB mounted microSD card. At the conclusion of exercise, data was uploaded to a personal computer via USB for analysis.

Measurement of Energy Expenditure

Energy expenditure was measured via indirect calorimetry using a fully automated, validated metabolic measurement system (Vmax Spectra. CareFusion, Yorba Linda, CA)²⁰. Each subject was instructed to breathe through a mouthpiece affixed to a hot

wire flow transducer to determine expired air volume breath-by-breath. A sampling tube coupled with the flow transducer carried samples of the expirate to oxygen (O_2) and carbon dioxide (CO_2) analyzers for determination of exhaled gas concentrations. Volume and gas concentrations measured were time aligned for calculation, display, and recording of oxygen uptake ($\dot{V}O_2$), carbon dioxide output ($\dot{V}CO_2$), and minute ventilation ($\dot{V}E$) breath-by-breath throughout each exercise bout.

Calibrations were performed on the day of and every hour while testing. Flow calibrations were performed with a 3-Liter calibration syringe, and gas calibrations were done with two standard gases. Since all measurements were recorded in a laboratory setting, ambient temperature calibrations were conducted at the beginning of each day.

Heart Rate

Heart rate was continuously recorded every 5 seconds with a heart rate monitor attached to a chest strap (RS400, Polar Inc. Lake Success, NY). Heart rate was time-synchronized with breath-by-breath data from the metabolic cart offline. Heart rate was monitored as a measure of exercise intensity relative to maximal heart rate and to ensure return of post exercise heart rate to resting levels prior to initiating exercise at every intensity in the treadmill and stepping matrix.

Statistical Analysis

Statistical analyses were carried out using R version 2.12.2.

Data recorded from each PAM device was separated by each of the nine intensities for both treadmill and stepping exercise. PAM data was then time-synchronized with data recorded from the metabolic cart. Oxygen uptake during minutes 4-6 was examined to verify the presence of steady state for all intensities. Coefficients of variation were calculated for all oxygen uptake measured during this defined period. Steady-state $\dot{V}O_2$ (L/min) was defined as the mean $\dot{V}O_2$ during the last two minutes of each 6-minute bout of exercise.

The steady-state $\dot{V}O_2$ was converted to energy expenditure (EE, kcal/min) using the following equations:

$$\frac{kcal}{min} = \frac{kcal}{L O_2} * \frac{L O_2}{min} \quad (Equation 1)$$

$$\frac{kcal}{min} = \left(1.232 * \frac{\dot{V}CO_2}{\dot{V}O_2} + 3.8149 \right) * \dot{V}O_2 \quad (Equation 2)$$

EE is derived by converting the ratio of carbon dioxide output to oxygen uptake (respiratory quotient during steady state exercise) to calories per liter of oxygen as determined by the thermal equivalents of oxygen for the non-protein respiratory quotient, and then multiplying by $\dot{V}O_2$ (L/min) for energy expenditure in kcal/min²¹.

Integrated steady-state activity (ΣA) was derived by the root of sums for squared average acceleration vectors for each axis (x,y,z) from minutes 4-6 (Equation 3). This calculation applies Pythagoras's theorem to derive a vector magnitude based on the sum of squares of the individual axes.

$$\text{steady state PAM activity counts} = \sum_{t=4}^6 \sqrt{\bar{x}^2 + \bar{y}^2 + \bar{z}^2} \quad (\text{Equation 3})$$

ΣA for each PAM was analyzed in 7 different configurations: left ankle (ΣA_{LL}), right ankle (ΣA_{RL}), left wrist (ΣA_{LA}), right wrist (ΣA_{RA}), both ankles (ΣA_{BL}), both wrists (ΣA_{BA}), all limbs ($\Sigma A_{BL,BA}$). ΣA for each configuration was plotted against energy expenditure for each of the nine intensities for treadmill and stepping exercise. Instead of utilizing linear correlations for EE versus ΣA , which only accounts for error on the abscissa via the least squares method, orthogonal correlations (r^2) were sought to account for error on both graphical axes for each of the seven PAM configurations.

A one-way ANOVA was used to determine the presence of statistically significant differences between the r^2 values for the seven PAM configurations for all 10 subjects. However, since the requirements for conventional one-way ANOVA require a balanced design, normal distribution, and equal variances among the group, ANOVA was conducted along with bootstrap methods. The test statistic was designed to detect significant differences ($\alpha=0.05$) comparing the calculated “F-like” statistic with a modeled “F-like” statistic calculated from 1,000 resampling trials for each of seven configurations. This “F-like” statistic is a modification of the original equation, in which the “sum of squares” has been replaced with the “sum of absolute values”. Group medians were used in the calculation of the F-statistic due to the lack of normal distribution in the data. This F-statistic was then compared to a 95% confidence interval generated from the pool of resampled F-statistics. F-statistic values within the 95% confidence interval represent values calculated from trials in which random samples of

the original dataset do not demonstrate significance. In other words, the validity of the null hypothesis of this subset of data (H_0 = no difference in percentage of variability explained between all seven PAM configurations) by producing a range of possible values of the F-statistic through random sampling of values from each PAM configuration can be determined.

Two-factor ANOVA was used to quantitatively assess the effect of both speed and grade on EE and ΣA measured at the left arm. This PAM configuration is consistent with physical activity monitoring trends focused on wrist-mounted accelerometer orientation. The conventional two-factor ANOVA was approached with bootstrapping methods due to violations of the same three basic assumptions described with the one-way ANOVA, along with the presence of unbalanced design due to missing data points. However, unlike the one-way ANOVA, the interactions and effects of both speed and grade on the dataset needed to be examined. For that reason, the two-factor ANOVA used in this analysis was modeled to examine the effect of speed and grade separately, then a combined effect of the two on energy expenditure and PAM activity counts. This was achieved by calculating the “F-like” statistics for speed (FA), grade (FB), and interaction of speed and grade (FAB). This test statistic was a modification of the conventional F-statistic by substituting the squared values within the equation with absolute values. To eliminate the consequences of unequal variances of the groups during bootstrapping, the original dataset was de-meant from the grand mean of the dataset. Columns and rows within the original dataset were also de-meant prior to bootstrapped ANOVA to examine the effect of speed and grade separately while preserving column and row

means. De-meaning the data prior to bootstrapping maintains the integrity of the variances within each group. Additionally, comparing the calculated F-like statistic with the boot-strapped F-like statistic minimizes the need for conventional formulas to be used; therefore, valid comparisons can be made between the calculated and modeled test statistic.

The same statistical approach was used for stepping exercise, with “F-like” statistics calculated for step height (FA), step rate (FB), and interaction of step height and rate (FAB)

Results

All subjects completed the exercise protocol; however, for the 5 mph portion of the treadmill protocol, data from three subjects at 0% grade and two subjects at 2.5 and 5% grade had to be discarded due to either an error in PAM configurations or inability to run at this speed. One subject did not complete the 20 inch step at 24 and 30 steps/minute due to acute knee pain.

Synchronization between metabolic data and PAM output was successful. An example of this synchronization is seen in Figure 4 for one subject during one treadmill intensity. Minutes 4-6 (seconds 240-360 of the top panel) and corresponding acceleration vectors (bottom panel) for all three axes were defined as the steady-state period. An example of the distribution of oxygen uptake for treadmill and stepping exercise is shown in Figure 5 and Figure 6, respectively. All steady-state periods for nine intensities of treadmill exercise performed by each subject had coefficients of variation (CV) ranging from 0.02

to 0.34. For stepping exercise, CV ranged from 0.02 to 0.36. Four instances of treadmill exercise and one of stepping exercise were not considered to reflect steady state (due to measured oxygen uptake with a CV larger than 0.25) and were thus discarded from further analysis.

Figure 7 and Figure 8 depicts the relationship between ΣA and EE for treadmill and stepping exercise. For treadmill exercise (left panel), a stepwise pattern is evident. The bottom left cluster represents 2.5 mph walking; the middle cluster represents 4.0 mph, and the top cluster represents 5.5 mph, with subsequent increases in grade at every cluster. Specifically, two important observations can be made: a) EE is sensitive to increases in speed and grade b) ΣA is sensitive to increases in speed, but not grade.

To test for robustness of the relationship between EE and ΣA , EE was plotted for all intensities against ΣA , both averaged for all subjects, revealing strong correlations. The median and mean r^2 values calculated from orthogonal correlations derived from the seven PAM configurations for ΣA and EE are displayed in Table 4.

One-way ANOVA was performed, as specified in Methods, for the purpose of detecting any significant differences in PAM configurations (ΣA_{LL} , ΣA_{RL} , ΣA_{LA} , ΣA_{RA} , ΣA_{BL} , ΣA_{BA} , $\Sigma A_{BL,BA}$). Bootstrapping, rather than conventional one-way ANOVA, was necessary for two reasons: a) the distributions for all seven PAM configurations were negatively skewed for both treadmill and stepping exercise (Figure 9 and Figure 10) and b) the data also contained unequal variances across all groups, ranging from 0.003 to 0.03. Additionally, due to the first reason above, the median was the test statistic of choice.

The F-statistic for treadmill exercise was determined to be 0.42, which lies within the 95% confidence interval (0.14 to 0.74) of 1,000 F-statistics calculated from a de-mediated, shuffled dataset. With a $P < 0.05$, no significant differences can be detected, given the current dataset. For stepping exercise, the F-statistic was calculated at 0.26, well within the 95% confidence interval (0.15 to 0.84).

For treadmill exercise, two-factor ANOVA was conducted to examine the effects of both speed and grade, dependently and independently, on energy expenditure. F-like statistics were calculated examining the effect of speed ($F_A = 2.35$, $P = 0.06$), grade ($F_B = 0.69$, $p = 0.101$), and speed and grade interaction ($F_{AB} = 2.2$, $P = 0.073$), compared to a pool of generated F-like statistics via bootstrap (Figure 13).

Two factor ANOVA was similarly performed for PAM activity for each of the 7 configurations. F-like statistics were calculated examining the effect of speed, grade, and the interaction of both speed and grade (Table 6), compared to a pool of generated F-statistics via bootstrap. Examples of the confidence intervals generated from the bootstrap pool for PAM activity measured from the left arm and right leg are shown in Figure 15 and Figure 17, respectively. Similarly, stepping exercise was analyzed in the exact same manner. F-like statistics from two-factor ANOVA on energy expenditure were calculated for the effect of height, rate, and height and rate interaction, shown in Table 7, and compared to a pool of generated F-like statistics via bootstrap. Confidence intervals for energy expenditure are shown in Figure 14.

Again, two factor ANOVA, calculated for PAM activity for all 7 configurations, yielded F-like statistics for the effect of height, rate, and height and rate combined, shown in Table 7, and were compared to a pool of generated F-statistics via bootstrap. Examples of the confidence intervals for left arm and right leg are shown in Figure 16 and Figure 18.

Two factor ANOVA, calculated for PAM activity for the right leg, yielded F-like statistics for the effect of height ($F_A = 1.92$, $p = 0.15$), rate ($F_B = 1.98$, $p = 0.05$), and height and rate combined ($F_{AB} = 1.43$, $p = 0.15$), compared to a pool of generated F-statistics via bootstrap (Figure 23).

Study 2. Interrelationship between Accelerometry, Heart Rate and Energy Expenditure

The second part of this study was aimed at exploring the relationship between heart rate and tri-axial accelerometry which we have chosen to call the "Cardiocaloric Index" (CCI) from a single accelerometer during an incremental workrate treadmill running protocol. Our approach for this part of the study was to apply a chest-mounted physiological monitor which includes a single tri-axial accelerometer during a standard incremental treadmill test and compare the heart rate and accelerometer relationship with chronotropic index.

Subjects

For the second part of the study, 10 different subjects (all men) were recruited to perform three maximal incremental treadmill exercise tests. Their characteristics are

shown in Table 8. All subjects recruited for this part of the study were physically active according to American College of Sports Medicine criteria, performing five or more days per week of greater than 30 minutes per day of moderate exercise. Subjects were instructed to refrain from caffeine and physical activity for 24 hours prior to laboratory testing. A light meal prior to the testing session was recommended.

Methods

Exercise Protocol

In concert with ongoing research in our laboratory, the Wellness Fitness Initiative (WFI) treadmill protocol, updated in 2008, was deemed most appropriate for this study. It is one of the essential fitness tests within the Fire Service Joint Labor Management Wellness Fitness Initiative, created by a joint task force between the International Association of Fire Fighters and International Association of Fire Chiefs. After a 3-minute warm-up period at 3 mph and 0% grade, the treadmill workrate (\dot{W}) was increased in linear fashion by increasing speed and grade alternatively every minute (Table 9). A slight modification was made to this protocol at the first stage: grade was set to 1% elevation instead of 0% for a non-zero \dot{W} between minutes 3:01 and 4:00.

Subjects were instructed to continue exercise until volitional fatigue, and then were seated on a chair atop the stationary treadmill belt for 2 minutes to monitor heart rate recovery.

On the days of testing, subjects were instructed to report to the laboratory at approximately the same time of day. After every treadmill exercise was performed, each subject was monitored until their heart rate had returned to baseline (resting) levels prior to continuing.

Instrumentation

Physical Activity Monitors

Four PAM devices were again utilized for the second experiment and oriented in the same manner as for the first experiment. Data analysis was not present in this thesis.

Zephyr Bioharness™

A chest strap (Bioharness™ BT, Zephyr Technology Corp. Annapolis, MD) was worn around the chest below the nipple line. The Bioharness™ BT is programmed to record physiological variables such as heart rate, breathing rate, galvanic skin temperature, and activity in one-second epochs. Activity was measured in g-force as vector of magnitude units (VMU). VMU, derived over 1-second epochs using Equation 3, represents a change in acceleration without a directional component. Minimum and maximum values of x, y, and z acceleration were also recorded but not used in the present analysis.

Measurement of Energy Expenditure

During the incremental treadmill protocol oxygen uptake was directly measured by exhaled gas analysis using a metabolic measurement system (Oxycon Pro, Carefusion, Yorba Linda, CA) which has been validated for measuring minute ventilation, oxygen uptake and carbon dioxide output with the Douglas bag method across various exercise intensities²². Each subject wore a close-fitting facemask. Flow was measured using a turbine transducer attached to the facemask. Exhaled gas concentrations were continuously sampled and time-aligned with the flow signals to measure oxygen uptake and carbon dioxide output. Breathing frequency, $\dot{V}O_2$, $\dot{V}CO_2$, and tidal volume were recorded at each breath for the duration of exercise.

Flow and gas calibrations were performed every day before each exercise test. Since all measurements were recorded in a laboratory setting, ambient temperature calibrations were conducted at the beginning of each day.

Heart Rate

Continuous heart rate monitoring was provided before, during, and after exercise using a 12-lead electrocardiograph coupled to the Oxycon Pro metabolic cart. Heart rate was recorded with breath-by-breath measurement from the metabolic cart. Heart rate was monitored prior to testing in order to ensure that tests were initiated at or near resting values (<100bpm).

Additionally, heart rate was continuously recorded every second with the Zephyr Bioharness. Both heart rate signals were then time-synchronized with breath-by-breath data from the metabolic cart.

Statistical Analysis

Statistical analyses were carried out utilizing Matlab version R2011b and Microsoft Excel 2010.

Independent Variables

Twenty-eight independent variables total were extracted from each incremental exercise test and were organized in matrices, consisting of three columns corresponding to three trials performed, variable number of rows corresponding to exercise time (in breath-by-breath increments), and pages corresponding to the 10 subjects (Figure 3). An epoch length of 15 seconds was chosen for the analysis.

Of these 28 independent variables, heart rate from Oxycon Pro (HR.ox), heart rate from Bioharness (HR.bh), oxygen uptake ($\dot{V}O_2$), carbon dioxide output ($\dot{V}CO_2$), activity (VMU), breathing frequency from Oxycon Pro (BF.ox), and breathing frequency from Bioharness (BF.bh) were analyzed.

Derivation of Additional Variables: Work and Energy Expenditure

Work rate for each subject was derived from body weight, speed, and grade using the following equation:

$$\text{workrate} = g * \text{speed} * \sin(\text{angle}) * \text{body weight (Equation 4)}$$

Where g equals the gravitation constant 9.81 meters per second², speed is in units of meters per second, angle is expressed as the arctangent of grade, and body weight is measured in kilograms.

Finally, EE was derived from breath-by-breath metabolic data using the same calculations shown in Equation 2. A total of 10 independent variables of the original 28 were then used in the following analyses.

Heart Rate and Respiratory Rate Reliability

Since both heart rate and respiratory rate were measured by both Oxycon Pro and Bioharness™ during exercise testing, a simple comparison was made to ensure validity between the two instruments. T-tests with equal variances were used to detect statistical differences, along with Pearson's correlation. Bland-Altman plots were generated to determine the level of agreement within two standard deviations.

Validity of Integrated Activity Measures

In order to test the validity of integrated activity measures from Bioharness, the relationship between VMU and \dot{W} , as well as VMU and EE was explored.

Proof of Concept for Cardiacaloric Index

HR.bh were then paired against workrate (\dot{W}), VMU, oxygen uptake ($\dot{V}O_2$), and energy expenditure (EE) throughout the entire incremental exercise test, and then linear correlations were sought for these four relationships.

Reliability of CI and CCI

Slopes and intercepts derived from CI and CCI were then compared between subjects and between three repeated trials to examine inter-subject and inter-trial variability. Mean coefficient of variations were compared between CI and CCI. Single-factor ANOVA was used to determine statistical difference ($\alpha=0.05$) in between subject variability. Reliability was assessed with an intraclass correlation coefficient (ICC) as described by Shrout et al and Weir et al on a scale ranging from 0-1^{23,24}. Values closer to 1 represent higher reliability and lower variance.

$$ICC = \frac{\text{Between subject mean square} - \text{within subject mean square}}{\text{Between subject mean square} + (k - 1) * \text{within subject mean square}} \quad \text{Equation (5)}$$

where k represents the number of trials.

The ICC seemed more suitable for comparing CI and CCI slopes and intercepts, since it adjusts for the effects of the difference in scaling in variances between measurements. Slopes and intercepts from both CI and CCI from all 30 exercise tests were paired with orthogonal regression to detect correlation between the two. This regression model was again used to account for observational error on both dependent and independent variables.

For the final analysis, the slopes of chronotropic index were plotted against the slopes of cardioaloric index for all thirty exercise tests to examine the relationship between the two.

$$HR = CI(\dot{V}O_2) + b_1 \text{ Equation (6)}$$

where CI = slope and b_1 = intercept

$$HR = CCI(VMU) + b_2 \text{ Equation (7)}$$

Solving HR equations equal to each other would result in

$$CI(\dot{V}O_2) + b_1 = CCI(VMU) + b_2 \text{ Equation (8)}$$

Solving for CCI would result in:

$$CCI = \frac{CI(\dot{V}O_2) + b_1 - b_2}{VMU} \text{ Equation (9)}$$

$$CCI = \left(\frac{\dot{V}O_2}{VMU} \right) * CI + \frac{b_1 - b_2}{VMU} \text{ Equation (10)}$$

Reorganization of the two equations allowed us to mathematically deduce that pairing a linear relationship against another linear relationship would result in another linear relationship. In this case, the independent variable, CI, would determine the dependent variable, CCI, when it is multiplied by a slope coefficient of $\frac{\dot{V}O_2}{VMU}$ and added with a constant of $\frac{b_1 - b_2}{VMU}$.

Results

All subjects reported termination of each exercise test at volitional fatigue. No significant differences were found between mean endurance times of each of the three trials (2-

factor ANOVA, $P=0.76$). No significant differences were found between $\dot{V}O_2\text{max}$, derived by averaging last 15 seconds of the exercise test (2-factor ANOVA, $P=0.47$). The coefficient of variation across trial means for both endurance times and $\dot{V}O_2\text{max}$ was 6%.

Figure 25 shows a plot of heart rate measured by Bioharness (HR.bh) against heart rate measured by the Oxycon 12-lead ECG (HR.ox). A slope of 0.904 suggests that the Bioharness underestimated heart rate when compared to our 12-lead ECG. The mean coefficient of variation was 4.3%. Pearson correlation revealed significant correlation at 95% confidence ($P<0.0001$). A Bland-Altman analysis (Figure 26) portrays this discrepancy further with a negligible measured difference (bias = 2.6 ± 17.6 beats/minute) in heart rates between the two devices within a 95% confidence interval. After removing outlier heart rates recorded from subject 3 (trials 1 and 3) and from subject 4 (trial 3), mean bias was reduced to 0.64.

Similar plots were generated for breathing frequency for both devices. However, in Figure 27, a slope of 0.59 highly suggests that a proportional error in breathing frequency detected by Bioharness may have existed, when compared to breathing frequency from Oxycon Pro. The mean coefficient of variation was 10.3%. The Bland-Altman plot in showed a higher slope in the differences in breathing frequencies (0.26). However, 93.9% of all breathing frequencies recorded during exercise within the established confidence interval of differences (3.22 ± 16.48).

Given the error in the remaining 7.4% of HR.bh, HR.ox was substituted for HR.bh for exercise tests performed by subject 3 on trials 1 and 3 and subject 4 on trial 3.

\dot{W} increased linearly throughout the incremental exercise tests. Figure 29 shows \dot{W} increments for all 10 subjects for each of the three trials.

Linear correlations were derived with \dot{W} as the independent variable plotted against $\dot{V}O_2$ as the dependent variable (Figure 30). r^2 ranged from 0.86 to 0.95, indicating high correlations between the two variables. The mean coefficient of variation was 6%. Single-factor ANOVA for trial means revealed no significant difference ($P=0.95$).

For linear correlations between \dot{W} and VMU, all but one test had coefficients of determination above 0.7 (Figure 31). Slopes from these linear correlations were then analyzed. By grouping all subjects per trial, single-factor ANOVA revealed statistically significant differences ($P=0.046$). 2-factor ANOVA revealed significant differences between subjects ($P=0.0001$), but failed to detect significant differences between trials ($P=0.86$).

VMU and EE were analyzed again in a similar manner (Figure 32). Single-factor ANOVA revealed significant differences between subjects ($P=0.03$).

Furthermore, a high degree of correlation was found between HR and \dot{W} ($r^2>0.85$) for all exercise tests (Figure 33). No significant differences were found between trials, while between subject variability remained high ($P=0.04$).

Linear correlations between chronotropic indices (HR and $\dot{V}O_2$) were compared between subjects and between trials (Figure 34). The comparison of CI slopes for each of the 10 subjects across trials 1-3 are shown in Figure 35. Single-factor ANOVA revealed no significant difference among chronotropic index slopes averaged among trials ($P=0.93$). The intraclass correlation coefficient was 0.80.

Validity of the HR/VMU relationship across repeated trials was also sought (Figure 36). Slopes and intercepts derived from linear correlations between HR and VMU for each of the 10 subjects were compared separately across all three trials. Single-factor ANOVA (Table 13) with grouped cardioaloric index slopes revealed no significant difference ($P=0.66$). However, ANOVA did reveal significant difference (Table 14) between subjects ($P=0.01$). Slopes and intercepts are not shown to differ significantly between subjects ($P=0.66$, $P=0.68$ respectively). The intraclass correlation coefficient was 0.31.

A linear response was demonstrated for all subjects during all three trials. Figure 36 shows all plots of HR.bh against VMU for all 10 subjects for all 3 trials. A comparison of slopes derived from linear regression of HR.bh and VMU for both CI and HR/VMU is shown in Figure 37. This plot resulted in a small linear correlation between the two ($r=-0.33$). Orthogonal regression between both slopes yielded similar results ($r=-0.32$, $P=0.04$).

A summary of statistical analytical parameters are displayed in Table 15, comparing all of the aforementioned relationships.

The relationship between CI and CCI slope is portrayed in Figure 38.

Discussion

Accurate prediction of energy expenditure from accelerometers is desirable for the study of human activity. Since any particular activity is likely to be characterized by the specific movement of all four limbs, accelerometers were affixed to both wrists and both ankles. In the first study, integrated activity from each accelerometer correlated well with energy expenditure calculated from measured oxygen uptake for both treadmill and stepping exercise.

Orthogonal regression was used in place of standard linear regression for determining the best fit line for all seven PAM configurations measured at steady-state energy expenditures for the nine treadmill intensities.

The coefficients of determinations (r^2) were compared with the goal of determining the best predictor of EE with the highest proportion of variability explained by the relationship between EE and ΣA . One-way ANOVA was conducted to test the null hypothesis that no significant difference between the seven PAM configurations was present in the given data. The value of our F-like statistic was found within the confidence interval generated by the 1,000 trials of possible F-statistics derived from resampled data. In other words, there exists a less than 5% chance that a difference could have been detected within the given dataset. This analytical approach does not demonstrate a significant difference between any of the seven PAM configurations in their ability to relate energy expenditure.

Since our data suggests that no statistically significant differences exist in the configuration chosen for measuring ΣA , an analysis of the left arm PAM activity during treadmill exercise was warranted in light of the recent National Health and Nutrition Examination Survey 2011-2014 support for wrist-worn accelerometers purposed for objective assessment of physical activity monitoring^{25,26}.

The nine treadmill intensities essentially represent a graded increase in work rate, as they are comprised of a combination of three speeds (2.5, 4, and 5.5 mph) and three grades (0, 2.5, and 5%). These combinations of speed and grade can be used to calculate work rate, using the equation¹⁶:

$$\dot{W} = 0.1634 * speed * \frac{grade}{100} * BW \quad (Equation\ 4)$$

where \dot{W} is work rate measured in watts, speed is in meters/min, and body weight (BW) in kilograms.

A linear relationship exists between work rate and oxygen uptake during incremental cycle ergometry¹⁴, and this relationship can apply to various other modes of exercise, such as treadmill exercise, based on known work rate efficiencies. Directly measured oxygen uptake can be converted to energy expenditure (in kcal/minute) by accounting for non-protein thermal equivalents (Equation 2). However, in addition, knowing the calculated work rate for treadmill exercise, one could estimate oxygen uptake, and therefore energy expenditure from treadmill speed and grade.

An important question is whether PAMs can detect the changes in speed and grade, for the purpose of more accurately predicting energy expenditure and ultimately refining current algorithms. In sum, three questions need to be answered:

- How does speed affect energy expenditure and PAM activity?
- How does grade affect the energy expenditure and PAM activity?
- Do both speed and grade interact to affect the data, i.e. does grade have an effect on changes in energy expenditure and PAM activity due to speed, and vice versa?

The left panel of Figure 19 shows a positive effect of speed on energy expenditure. As speed increases, energy expenditure increases. Also, increasing grade also results in an upward shift in energy expenditure. Given the parallel lines, however, an interaction between speed and grade may not be present. The right panel of Figure 19, in contrast does not reveal any grade effect for PAM activity for the left arm. It is also evident that increasing speed does increase PAM activity. Again, the right panel does not reveal an interaction between speed and grade. In both plots, a noteworthy observation lies in the increase in slopes after 4.0mph for all grades. This is most likely due to a change in mechanical efficiency from walking to running, which typically occurs above speeds of 4.0 mph.¹⁵

In stepping exercise, an increase in energy expenditure is evident for increases in both step height and step rate. The parallel lines in the left panel of Figure 20 suggest that no interaction may be present between step height and step rate on energy expenditure.

The right panel reveals an interaction effect for both step height and step rate at 24 and 30 steps per minute for PAM activity measured from the left arm. Additionally, for both left and right panels, step rates of 24 and 30 steps per minute elicit the largest range of energy expenditure and PAM activity. These data suggests that PAM accelerometers may not detect any significant change in activity at a step rate of 12 steps per minute. For PAM activity measured from the right leg, however, a small increase was observed at a step rate of 12 steps per minute among all step heights studied.

A quantitative analysis was provided by the two-factor ANOVAs analyses conducted on energy expenditure and PAM activity for the left arm. “F-like” statistics were calculated for speed, grade, and speed/grade interaction, then compared to a pool of 1,000 resamples of the original dataset in order to estimate the variability of the F-statistics. These F-statistics calculated for speed, grade, and speed/grade interaction, when paired with corresponding confidence intervals, help answer the three questions above. All F-statistics measured for energy expenditure reside within the generated confidence intervals. By examining the raw data itself, it is evident that increases in speed or grade increase steady-state energy expenditure. Therefore, it may be said that speed and grade, and their interaction are both statistically significant in influence energy expenditure. On the other hand, F_B for PAM activity counts, did lie outside the established confidence. This effectively demonstrates that the effect of grade on PAM activity did not result in a significant difference on PAM activity counts.

For stepping exercise, two-factor ANOVA was conducted in the same manner as above. Figure 16 and Figure 18 illustrate the effect of step rate on PAM activity measured by

the left arm and right leg, respectively, within the confidence interval, thus failing to reject the null hypothesis that differences in step rate can be detected.

We have demonstrated that energy expenditure prediction for all PAM configurations was robust throughout all intensities studied for both treadmill and stepping exercise. We also have shown that EE prediction shows high accuracy for speed-related increases (set at a constant grade) in treadmill exercise, but EE prediction is much weaker for grade-related increases due to weak interaction in our analysis between grade and EE. Similarly, for stepping exercise, EE prediction fared better with step height increases than step-rate increases due to the weaker effect of step-rate on PAM activity.

One advantage to our study is the novel approach of determining the effects of grade changes during repetitive activities such as treadmill walking. Melanson et al. reported similar findings from a study protocol that measured uni-axial accelerometry during treadmill walking and running at three different grades¹⁷. We have examined our approach qualitatively through the study of interaction plots between speed and grade on energy expenditure and PAM activity and quantitatively through two-factor ANOVA. The results from our 10 subjects, for the left arm PAM, are contrary to the guidelines of the NHANES experimental protocol for 2011-2014 on accelerometry and physical activity monitoring. The conclusion from our analyses is that grade (for treadmill exercise) and step rate (for stepping exercise) do not have a significant effect on PAM activity.

One of the possible weaknesses of the data could be the algorithm for determining activity level. Tri-axial accelerometers are able to accurately measure acceleration in three different axes; however, the current algorithm to utilize root-mean-squared values of all three axes for the purpose of quantifying motion into one representative acceleration vector may over-simplify this variable as a whole. In other words, one could surmise that analyzing the three axes separately may provide some indication of detectable grade increases during treadmill exercise. One could hypothesize, for example, that differences in acceleration might be detected in the sagittal plane during grade increases, as one may increase hip and knee flexion during walking or running, while simultaneously reducing forward acceleration in the lower extremities. Therefore, in future studies, similar data should be analyzed with sub-variables such as ΣA_x , ΣA_y and ΣA_z for the purposes of detecting the effect of grade changes during treadmill exercise for the purpose of accurately estimating energy expenditure.

Another possible weakness is the time-frame at which these accelerometers record and summate data. Most commercial accelerometers such as the Actigraph GT1M (Actigraph, Pensacola, FL), Actical (Bio-Lynx, Montreal, Quebec, Canada), and Tritrac R3D (Tri Trac Technologies Private, Ltd, Goregaon, Mumbai, India) determine activity in epoch data for the sole purpose of translating motion data into predictions of energy expenditure. These accelerometers, however, are purposed for long-term physical activity monitoring, and may be less sensitive to acute changes in motion such as treadmill grade changes. Accelerometers provided by the UCLA Wireless Health

Institute have the advantage of being fully customizable and capable of outputting raw-accelerometry data for deriving algorithms for energy prediction.

For the second study, our purpose for defining CCI as a new parameter for exercise testing is wholly dependent on two components: 1.) the accuracy of HR.bh 2.) reliability of VMU measurements over repeated trials. Therefore, our approach consisted of dissecting both of these components through rigorous statistical analysis and comparison to validated parameters.

Firstly, to investigate the repeatability of CCI, we determined that no significant difference in subject effort existed between all three exercise tests for each subjects with comparable endurance times and $\dot{V}O_2\text{max}$ (calculated as an average of the last 15 seconds of exercise) achieved during the WFI treadmill test. 2-factor ANOVA revealed high between-subject and low within-subject variability for these two measurements. The mean coefficients of variations (6%) further confirmed low variability between trials.

To validate Bioharness heart rate detection, heart rates recorded by Bioharness were compared to those obtained from a conventional 12-lead ECG. Clusters of data were spotted where heart rates were misaligned; these were speculated to be isolated tests in which heart rate had dropped spontaneously, and were unlikely due to a systematic error in Bioharness™ heart rate detection. Replacement of incorrect HR.bh with HR.ox at these clusters of outliers resulted in a marked improvement in the comparison between both heart rate sources. Therefore, we believe this justified our rationale to

address these outliers by pairing HR.ox with VMU for CCI for points at which HR.bh were outside the 95% confidence interval.

The differences in body weight among all completed subjects account for the variation in the pooled \dot{W} over time relationship in Figure 29. However, given the nature of the linear increase in \dot{W} throughout the incremental exercise test, variables of interest were paired with work rather than time. This analytical method standardizes the relationships examined by pairing select variables against a mechanical variable relative to subject body weight.

Analyzing the relationship between the two mechanical parameters (\dot{W} and VMU) was deemed important prior to studying their relationship to other physiological variables. Due to strong linearity between \dot{W} and VMU, we again found slopes derived by linear correlations between \dot{W} and VMU to be significantly different from subject to subject while similar in value for every trial per subject. Similar to $\dot{V}O_2$ and \dot{W} , a strong relationship between \dot{W} and VMU demonstrates validity in utilizing studying physiological parameters against VMU.

VMU exhibited a similar relationship when compared with EE. While our data for \dot{W} and VMU demonstrated a tight relationship between two mechanical variables, VMU was shown to be a valid measurement when compared with EE.

With HR and $\dot{V}O_2$ shown separately to correlate linearly with \dot{W} , pairing these two physiological measures result in a linear relationship with one another known as the

chronotropic index. HR and $\dot{V}O_2$ were shown to correlate well, given the linearity of both HR and $\dot{V}O_2$ with \dot{W} . Therefore, slopes and intercepts from regression equations derived for CI showed remarkable precision across all 3 trials, indicated by the low variance for most subjects and 91% agreement via intraclass correlation coefficient.

While strong linearity was demonstrated between HR and VMU for each subject at each trial, comparison of the slopes and intercepts derived from linear regression unfortunately did not yield positive findings. Significant difference was discovered between subjects, similar to slopes from chronotropic indices. Mean values for CCI slopes seem to be similar, as single-factor ANOVA did not detect any significant difference between trials. However, repeatability measurements for CCI slopes were less revealing, as agreement measured at approximately 59%.

Comparing the slopes of CI and CCI together did not result in a robust relationship as was previously hoped. A low coefficient of determination ($r^2=0.11$) from simple linear regression indicated a low correlation between CI and CCI. Modeling the data with orthogonal regression to account for two-dimensional error did not yield an improved relationship.

Given the linearity of the HR/VMU relationship, CCI seemed promising as a new metric initially; however the repeatability of this measurement did not seem to fare as well as it did with CI. Changing the range with which CCI was defined did not result in any improvement. Specifically, 15, 30, and 60 seconds were removed from both the beginning and end of exercise to determine if outliers at the endpoints caused some of

the variability; unfortunately, this only seemed to lessen the repeatability of CCI slopes between trials by introducing higher variances among subjects. Therefore, given the analytical approach that was used, we concluded that CI was not correlated with CCI.

Although the concept of the cardio-caloric index is in its infancy, it has potential to be a practical metric to demonstrate changes in cardiovascular fitness by pairing a commonly used parameter such as heart rate with a cheap yet accurate accelerometer. Newer, modern fitness apparatuses have upgraded simple heart rate monitors with peripherals such as global position systems, altimeters, and accelerometers. However, meaningful data has yet to be derived from tri-axial accelerometry data in relation to other physiological parameters.

Numerous studies (previously cited) have paved the way in integrating accelerometry data for the purposes of objective physical activity monitoring. However, given that this quantification also includes the collection and interpretation of non-rhythmic physical activity, we focused on collecting motion data during acute bouts of exercise. By utilizing accelerometers outfitted with other physiological monitors such as Zephyr BioHarness in a laboratory setting, we were able to quantify vectored motion specifically during standard exercise protocols such as step, walking, and running tests, ranging from steady-state exercise to maximal tests.

In theory, CCI may potentially simplify conduct of exercise tests by limiting the amount of cumbersome equipment that subjects are needed to wear. For example, mobile metabolic measurement systems pose as extra weight when worn during physical

activity, with face masks for expired gas analysis can add additional discomfort during testing. For these reasons, wearing a small, minimally-unobtrusive physiological monitor could reduce the overall subject discomfort during exercise testing.

Another advantage that CCI may have is its potential to derive clinically meaningful measurements from exercise tests performed at submaximal effort. Cardiovascular risk associated with exercise testing is at its highest upon fatigue during ramped protocols²⁷. Therefore, by limiting ramped protocols to submaximal effort, we could potentially derive clinically meaningful interpretations by comparing these established linear relationships and extrapolating meaningful data from them. From a laboratory safety perspective, we could mitigate the impact of these diagnostic tests on the incidence of adverse events.

Most importantly, the foundation of CCI must be tested rigorously with careful dissection of its components. Most importantly, VMU must be described as a valid and reliable parameter during treadmill exercise. Its relationship with other mechanical parameters (e.g. \dot{W}) must be solidified prior to extracting useful physiological measures from it.

As a new concept, cardiocaloric index was pilot tested with a small sample population with a limited range of physical conditioning and aerobic fitness. No power analysis was performed prior to study initiation, which may have contributed to the lack of significance found in several aspects of the study.

Future studies should be conducted to examine the effect of speed and grade, as well as their interaction on VMU.

Appendix A: Figures

Figure 1: PAM model X6-2 and axis orientation. (Gulf Data Concepts, LLC. Waveland, MS).

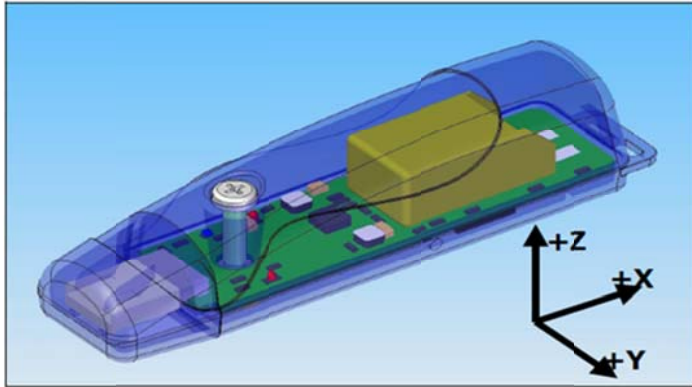


Figure 2: PAM Locations on extremities.

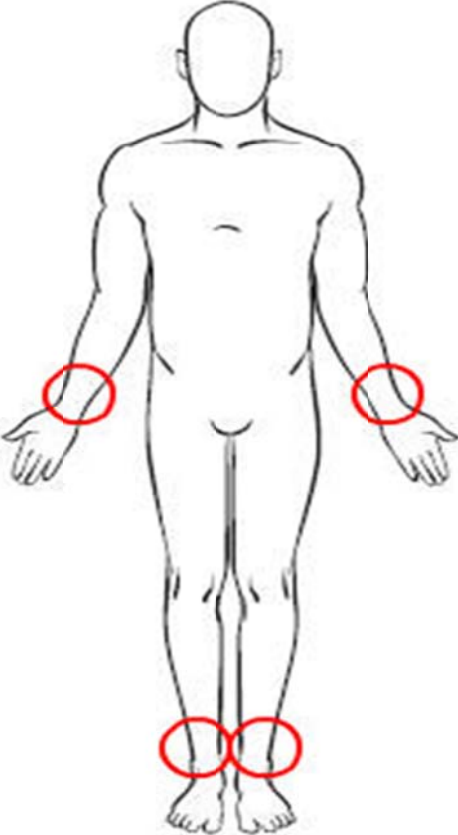


Figure 3: Variable organization in matrix format.

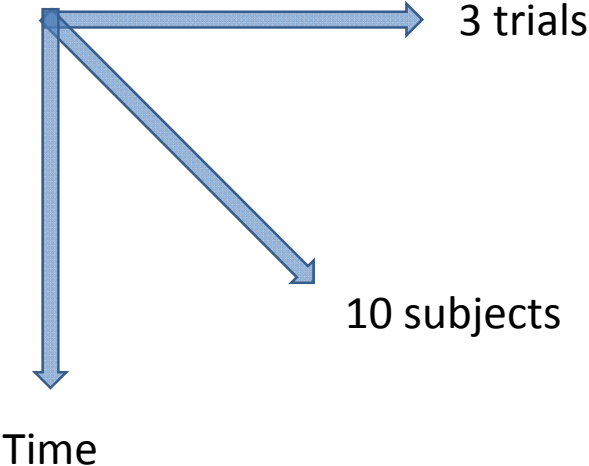


Figure 4: Example of time-synchronization between oxygen uptake and activity counts for one subject.

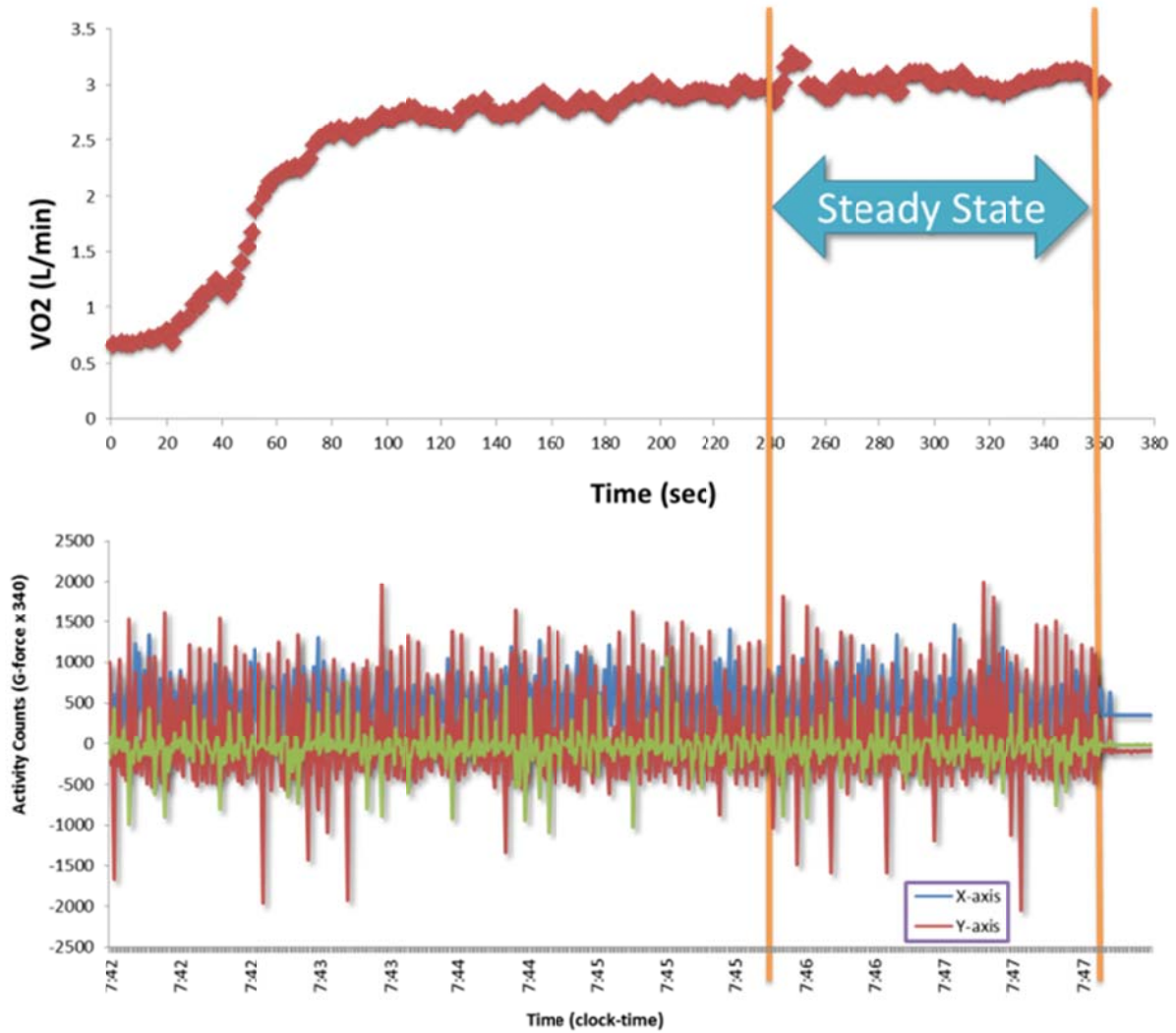


Figure 5: Stackplot of one subject's oxygen uptake during defined steady-state for all treadmill intensities (s1-s9).

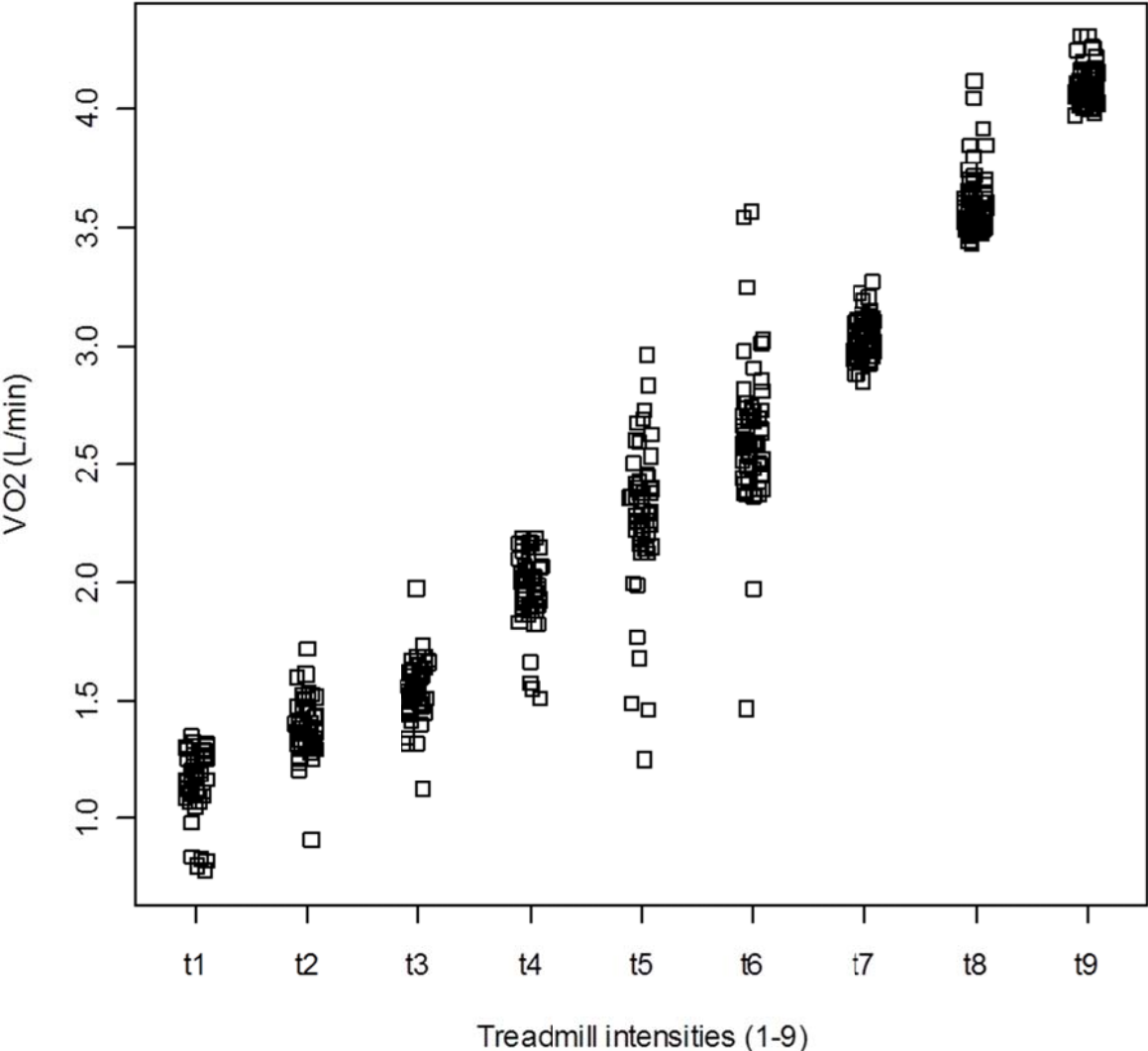


Figure 6: Stackplot of one subject's oxygen uptake during defined steady-state for all stepping intensities (s1-s9).

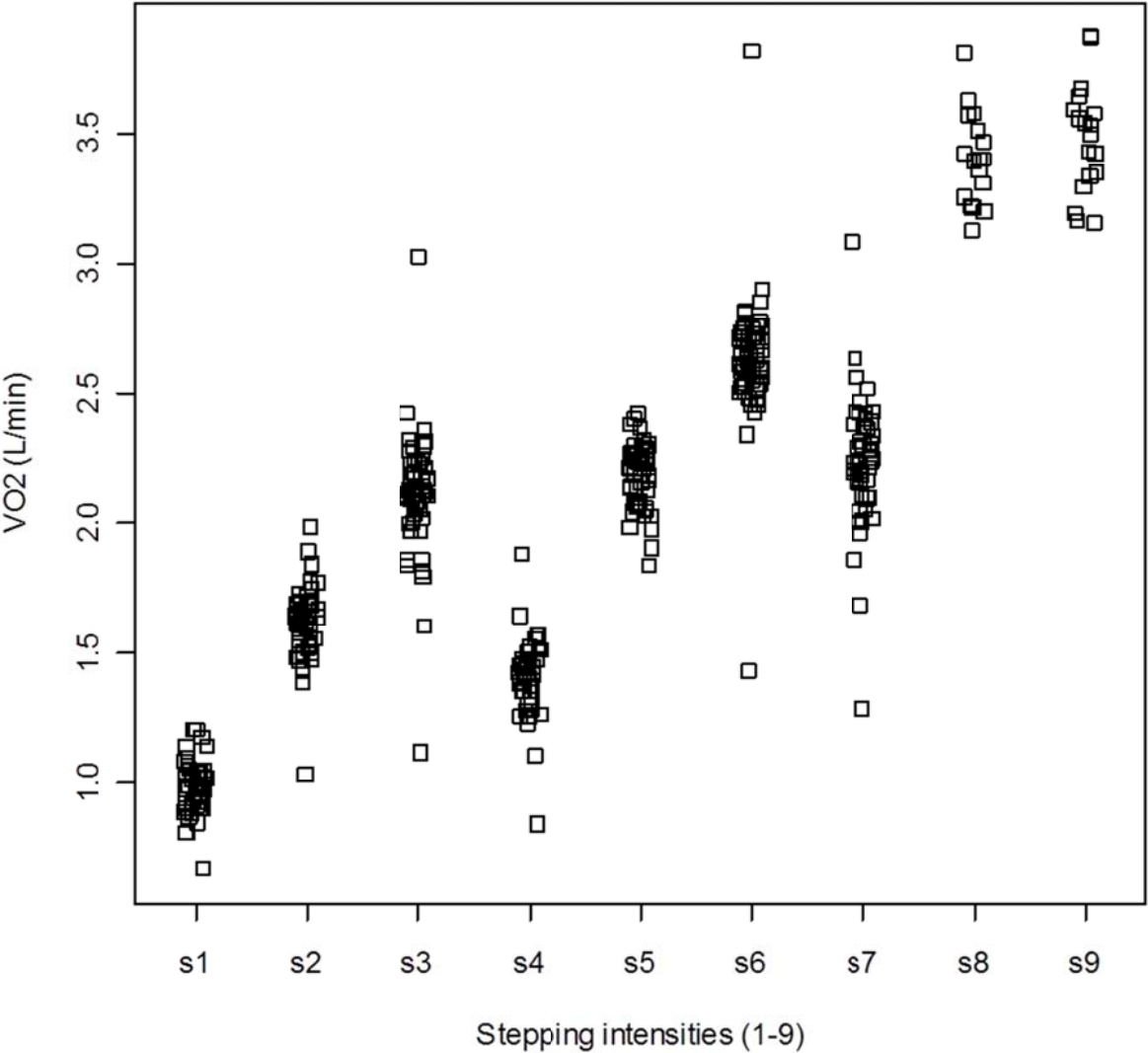


Figure 7: Integrated physical activity (ΣA) for all limbs plotted against energy expenditure for all treadmill intensities.

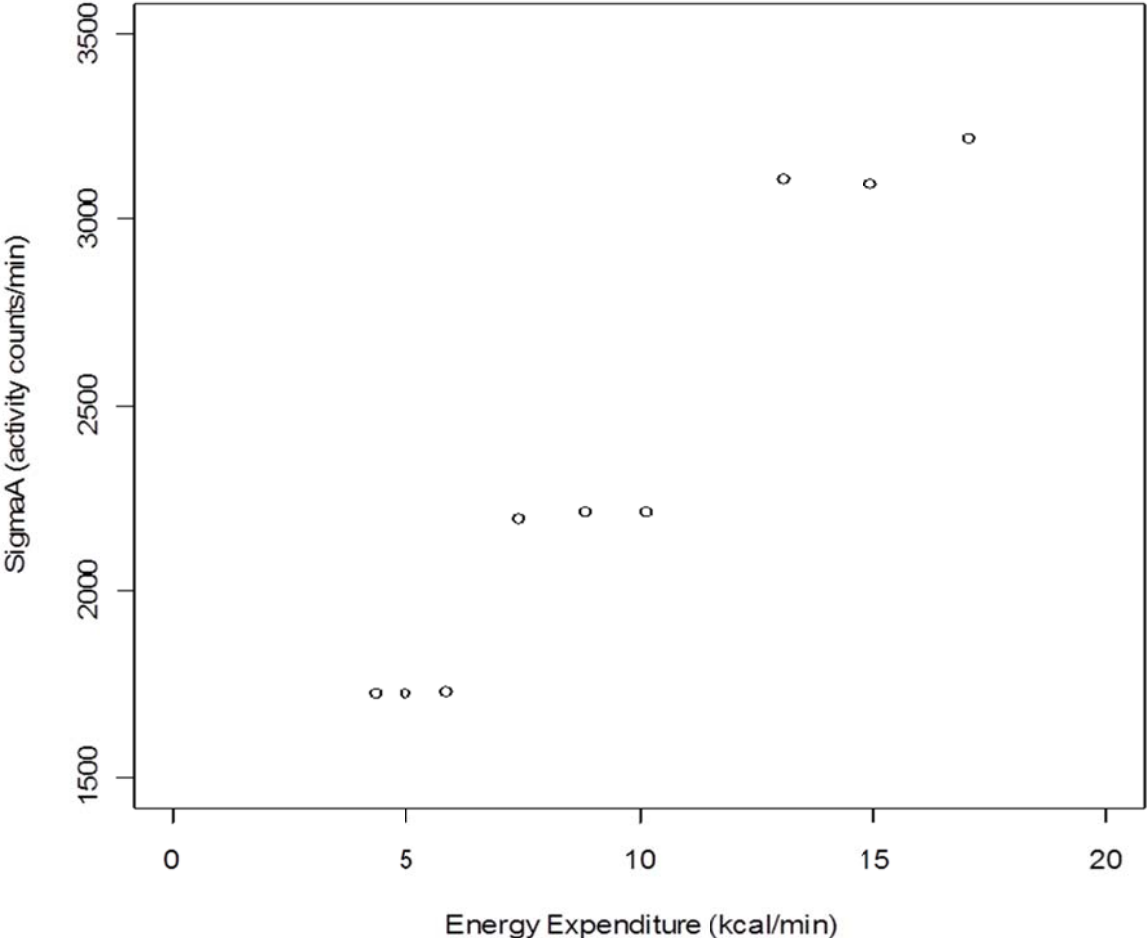


Figure 8: Integrated physical activity (ΣA) for all limbs plotted against energy expenditure for all stepping intensities.

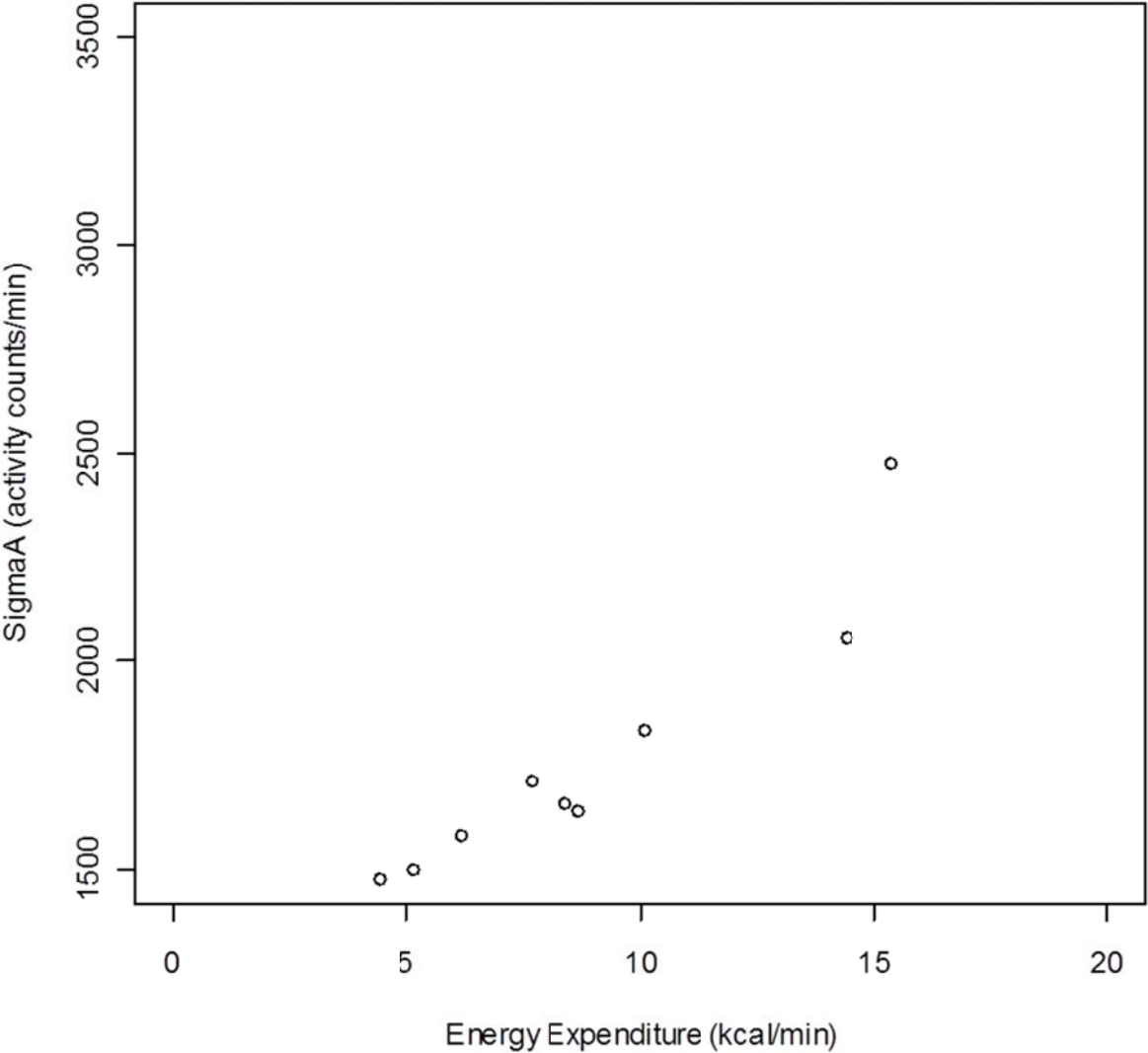


Figure 9: Stackplot of r² for seven different PAM configurations for treadmill exercise. LA=left arm, RA=right arm, BA=both arms, BL=both legs, AL=all limbs.

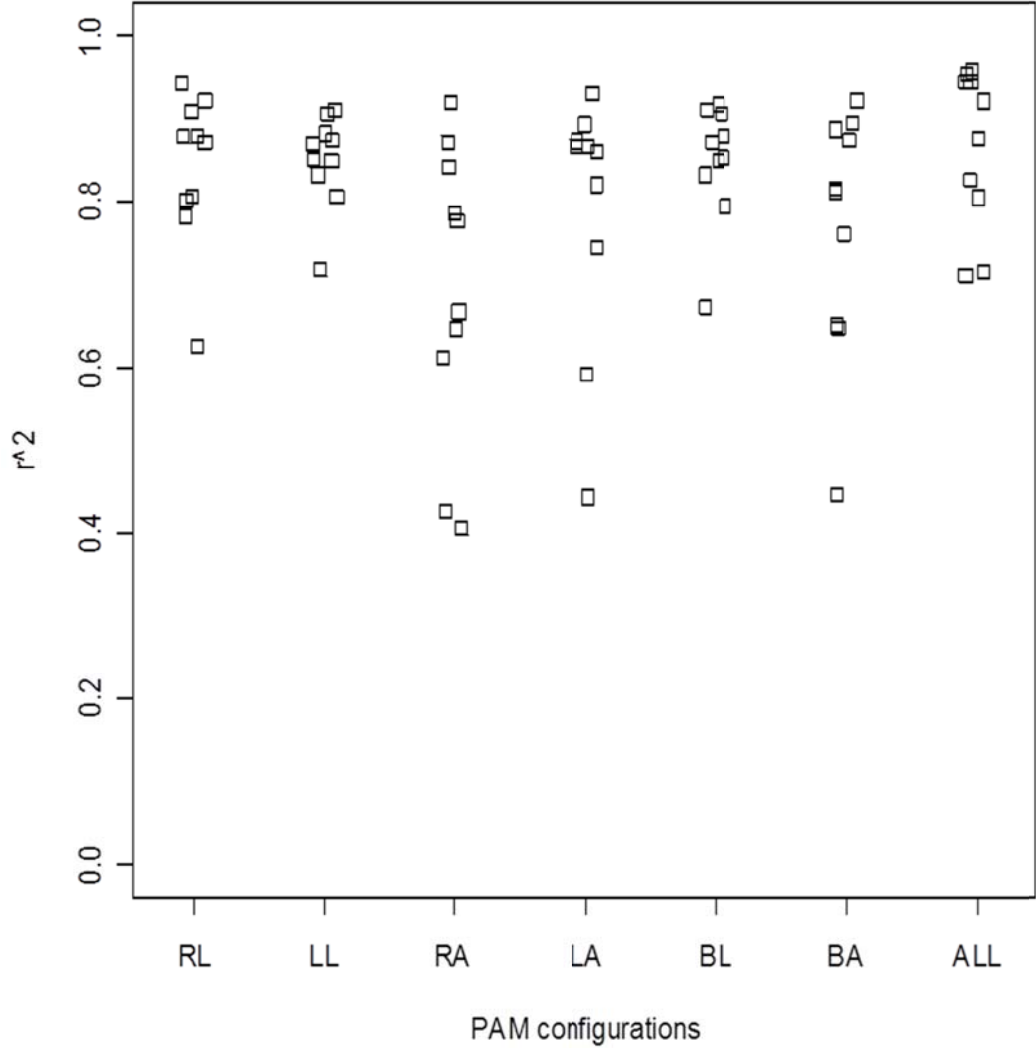


Figure 10: Stackplot of r^2 for seven different PAM configurations for stepping exercise. LA=left arm, RA=right arm, BA=both arms, BL=both legs, AL=all limbs.

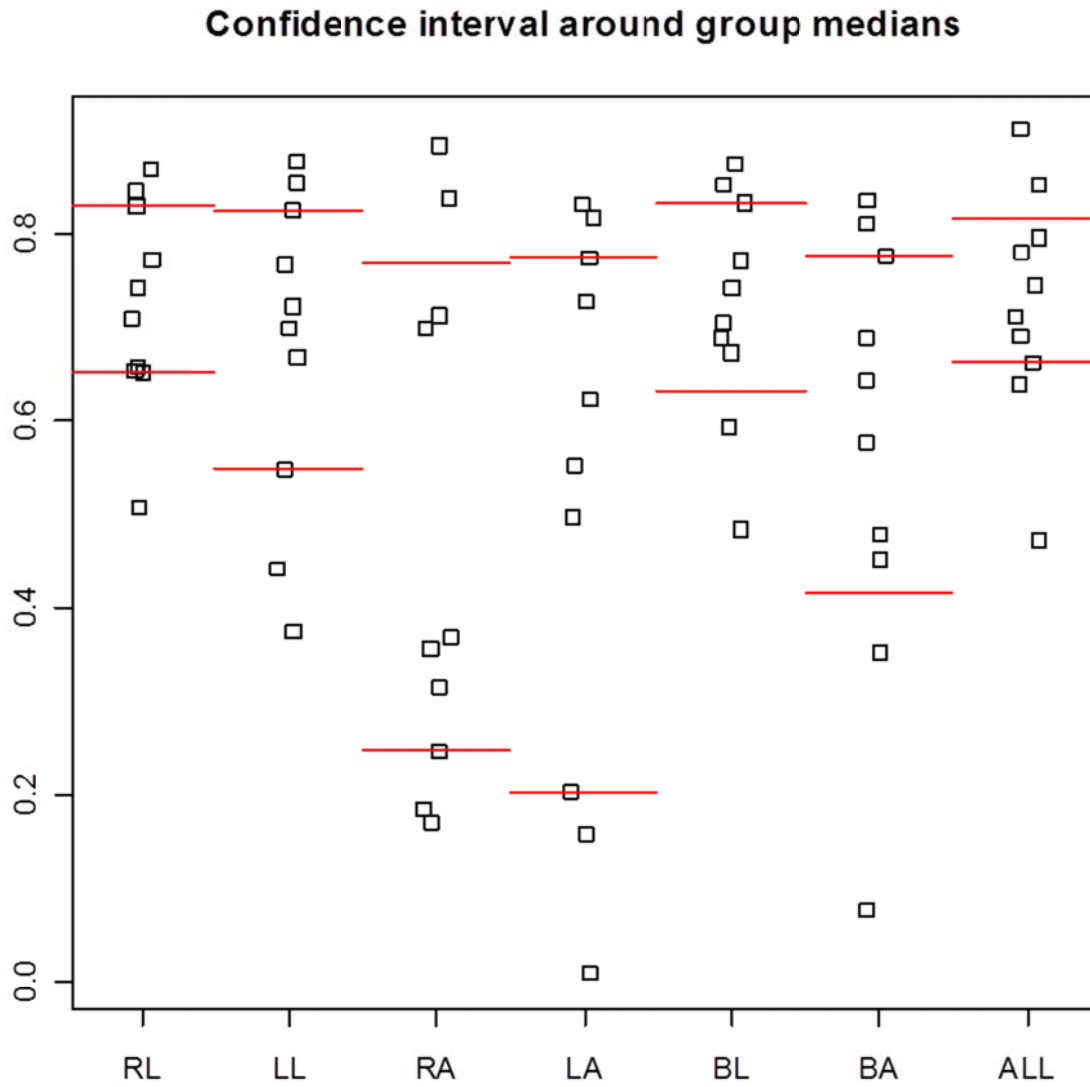


Figure 11: Distribution of simulated F-like statistics for treadmill exercise. (red line = calculated F-statistic. black vertical lines demarcate the 95% confidence interval).

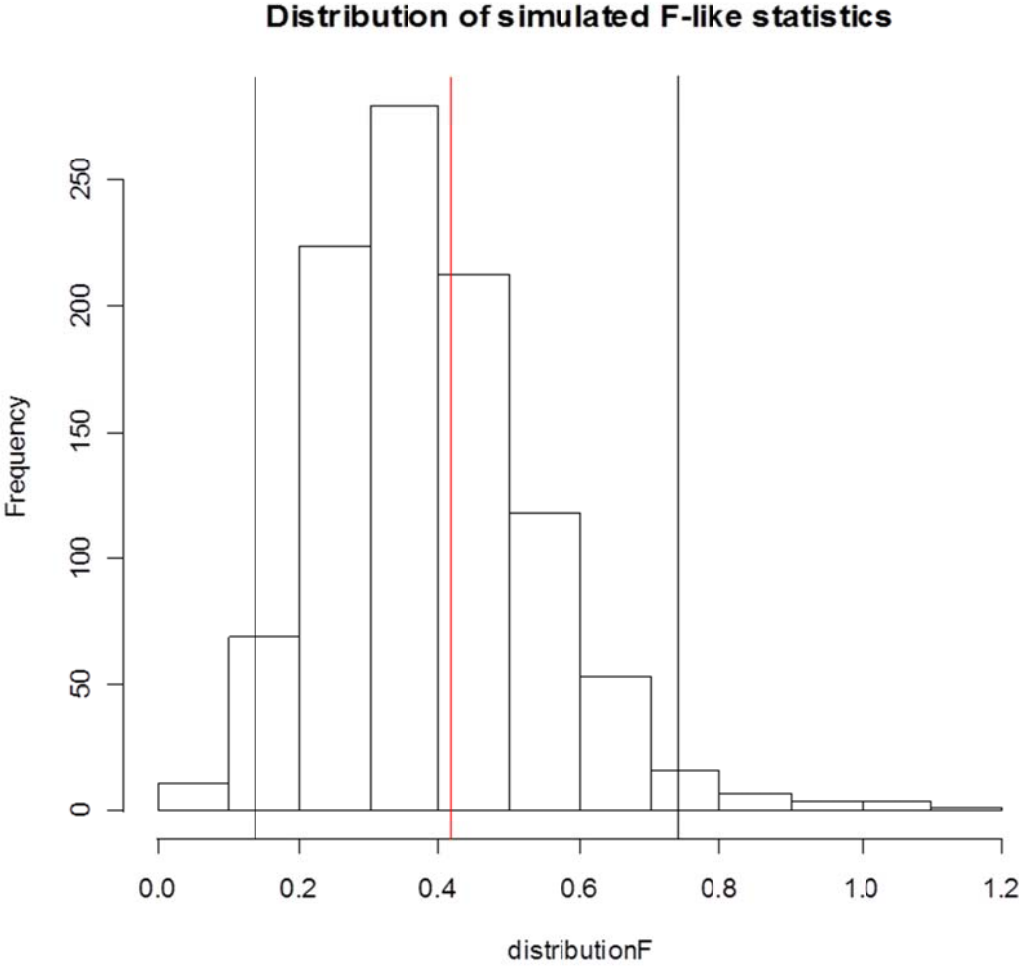


Figure 12: Distribution of simulated F-like statistics for stepping exercise. (red line = calculated F-statistic. black vertical lines demarcate the 95% confidence interval).

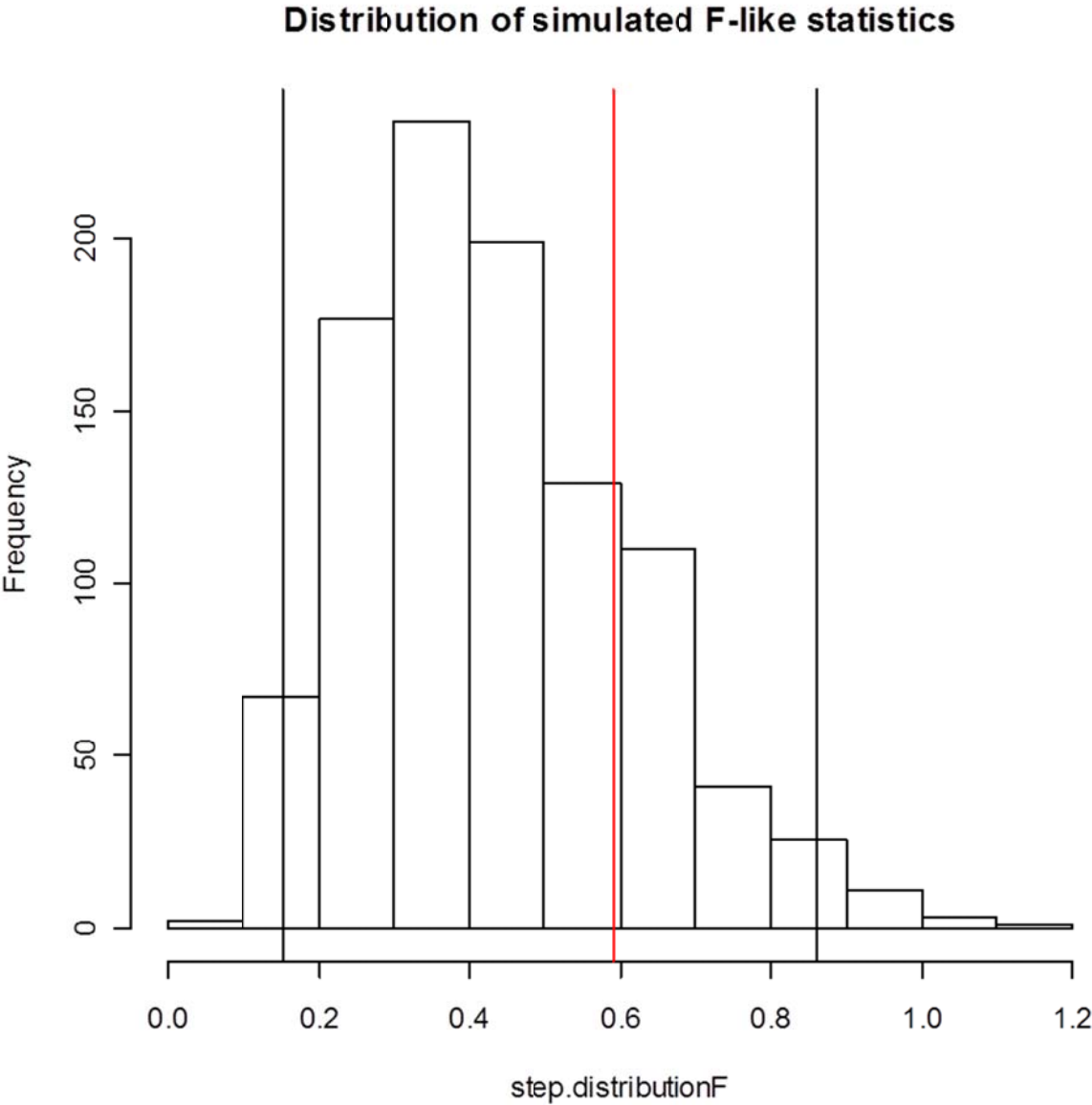


Figure 13: Confidence intervals for two-way ANOVA parameters for energy expenditure during treadmill exercise.

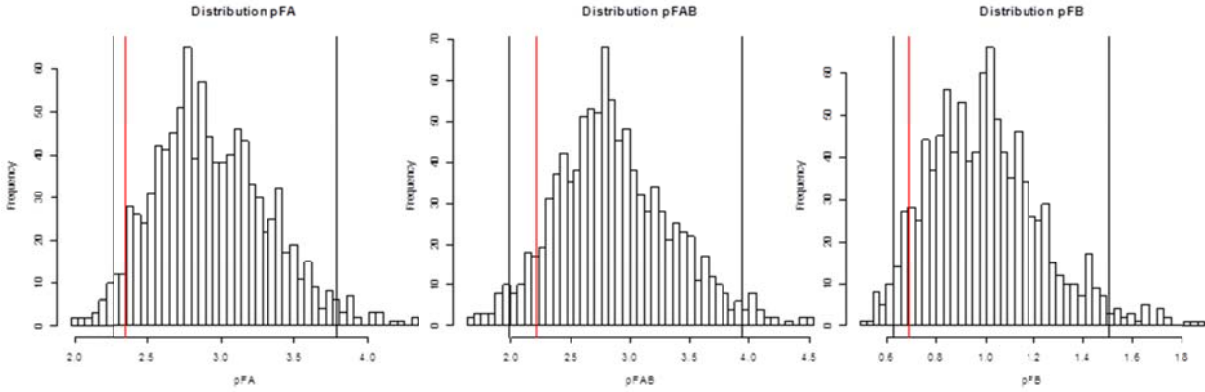


Figure 14: Confidence intervals for two-way ANOVA parameters for energy expenditure during stepping exercise.

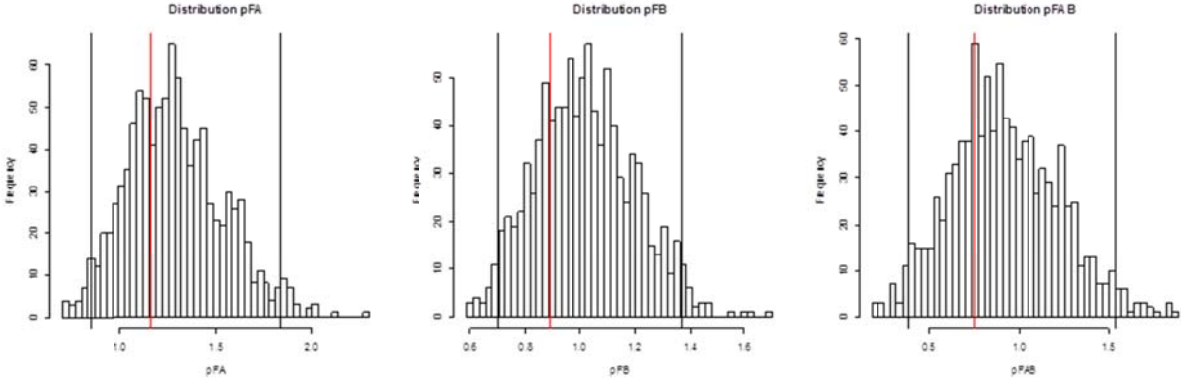


Figure 15: Confidence intervals for two-way ANOVA parameters for PAM activity counts (Left Arm) during treadmill exercise.

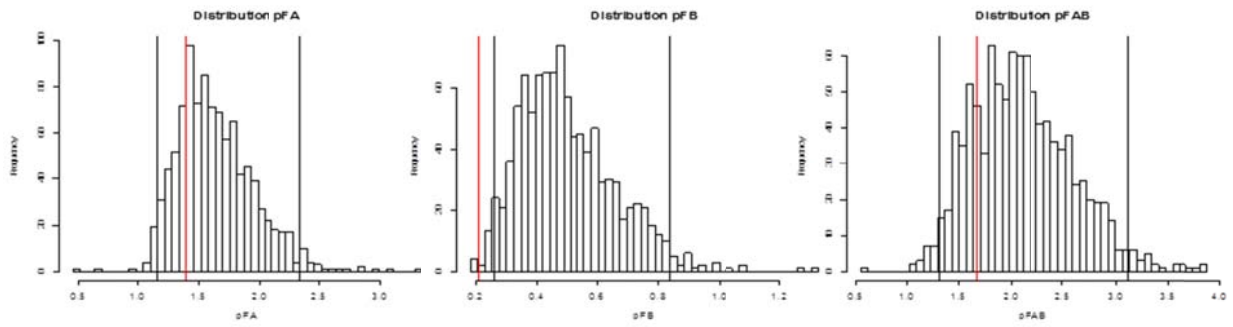


Figure 16: Confidence intervals for two-way ANOVA parameters for PAM activity counts (Left Arm) during stepping exercise.

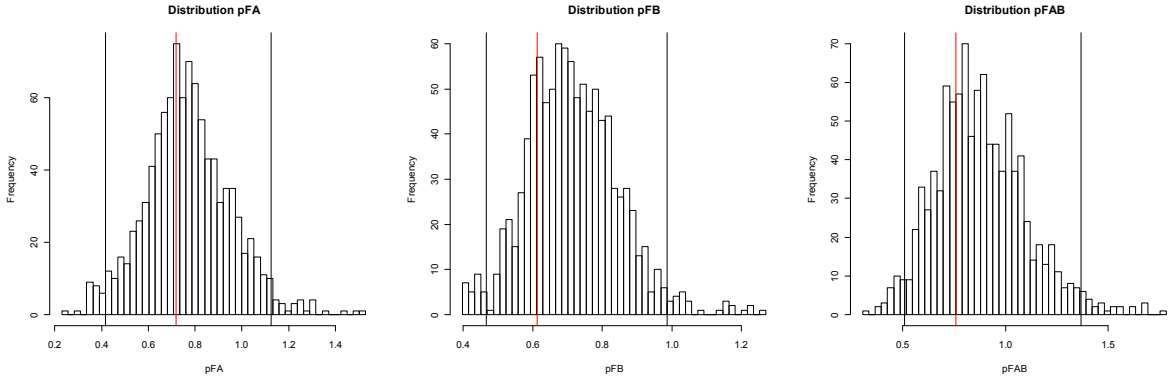


Figure 17: Confidence intervals for two-way ANOVA parameters for PAM activity counts (Right Leg) during treadmill exercise.

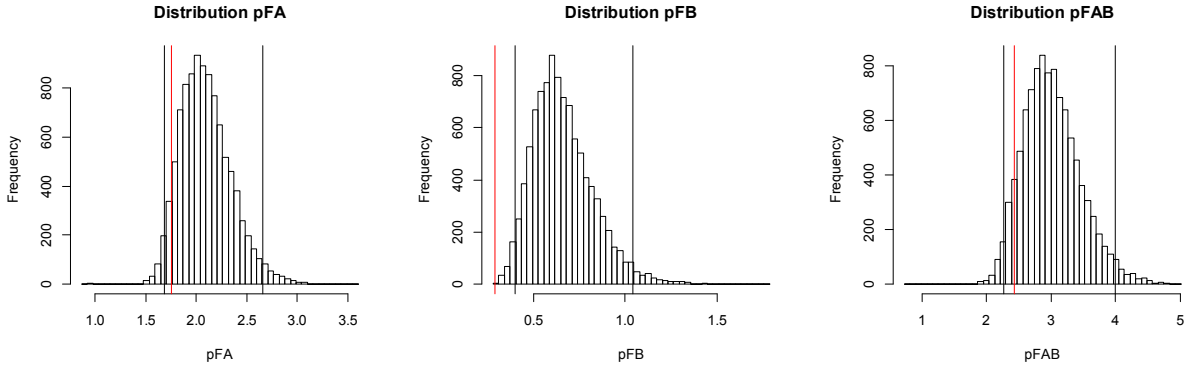


Figure 18: Confidence intervals for two-way ANOVA parameters for PAM activity counts (Right Leg) during stepping exercise.

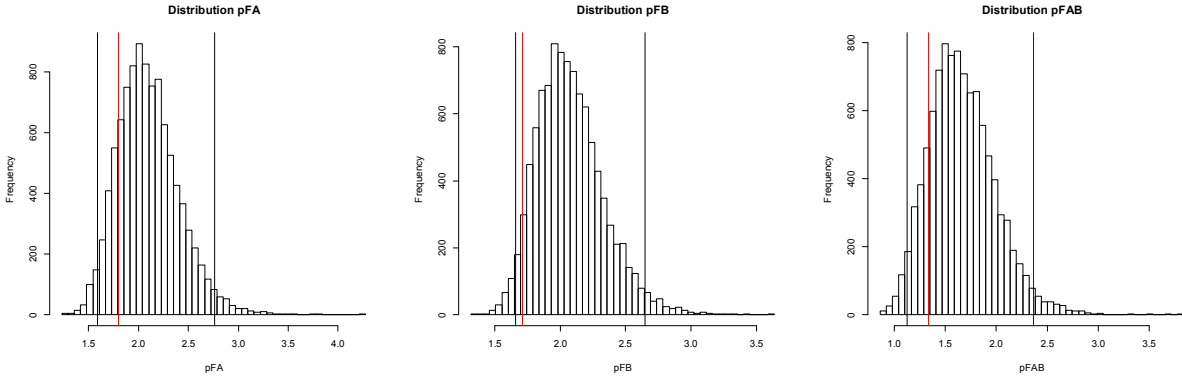


Figure 19: Estimated treatment means plot for both speed and grade on energy expenditure (left panel) and PAM activity counts for left arm (right panel) for treadmill exercise.

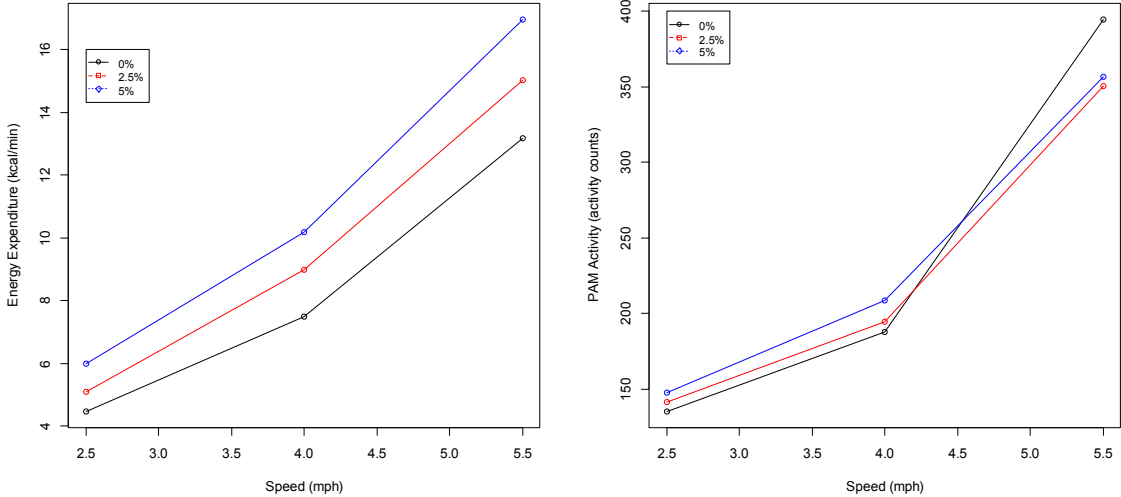


Figure 20: Estimated treatment means plot for both speed and grade on energy expenditure (left panel) and PAM activity counts for left arm (right panel) for stepping exercise.

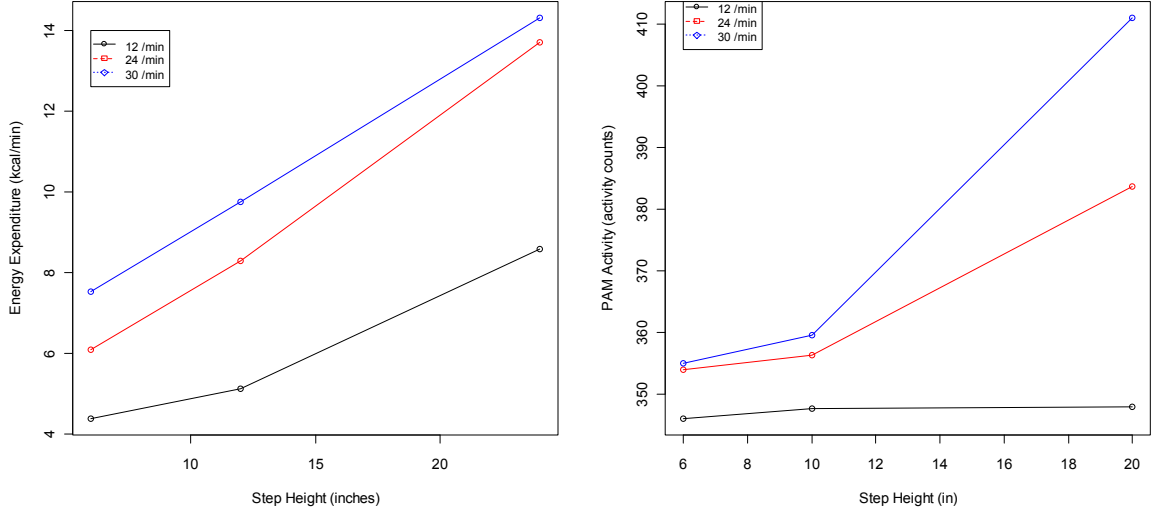


Figure 21: Estimated treatment means plot for both speed and grade on PAM activity counts for right leg for treadmill exercise.

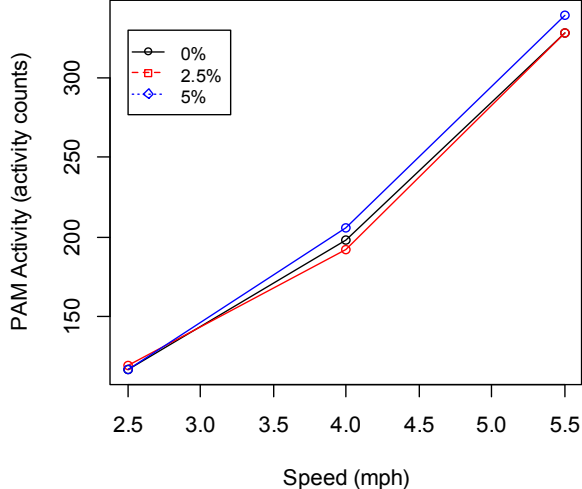


Figure 22: Estimated treatment means plot for both speed and grade on PAM activity counts for right leg (right panel) for stepping exercise.

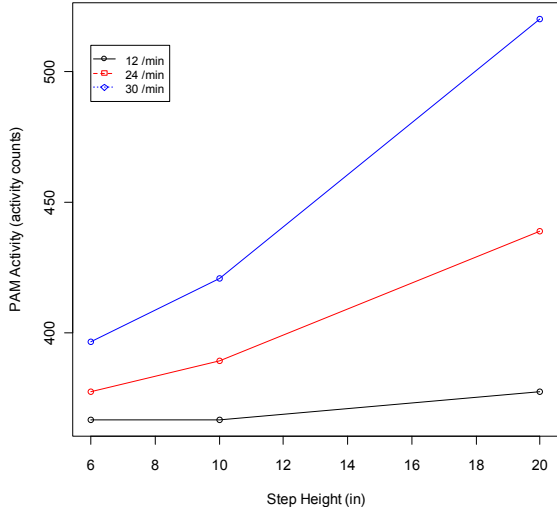


Figure 23: Confidence intervals for two-way ANOVA parameters for PAM activity counts (All Limbs) during treadmill exercise.

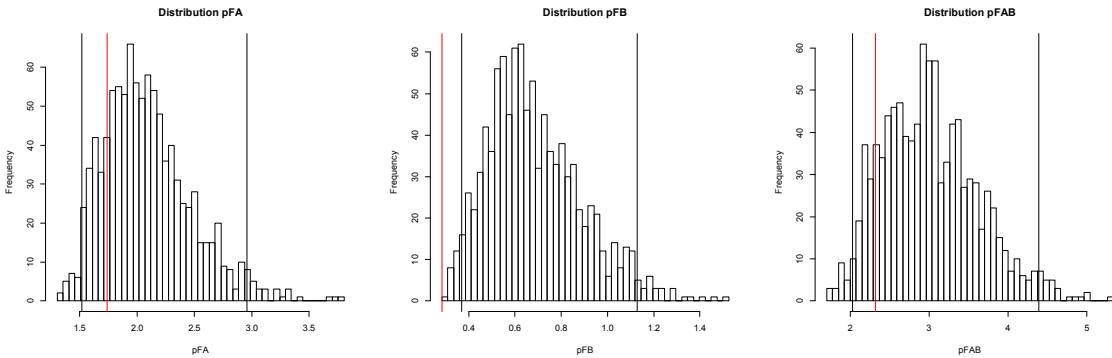


Figure 24: Confidence intervals for two-way ANOVA parameters for PAM activity counts (All Limbs) during stepping exercise.

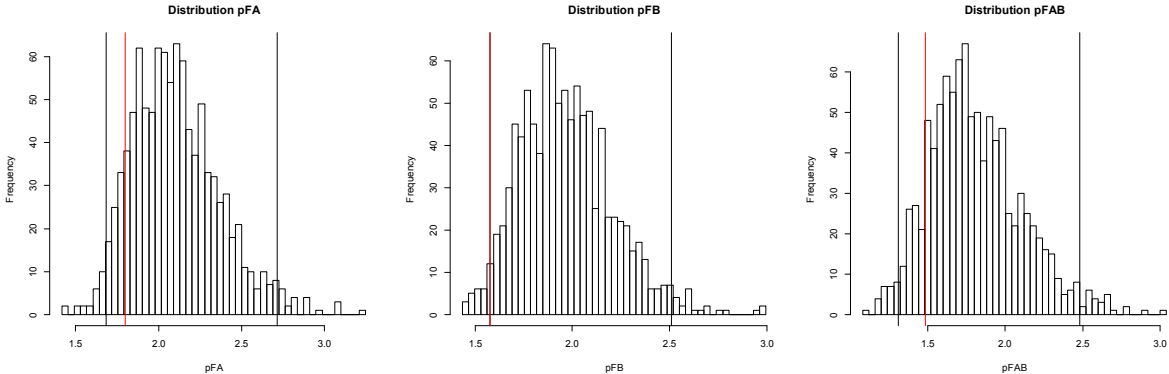


Figure 25. Paired heart rates for all exercise data.

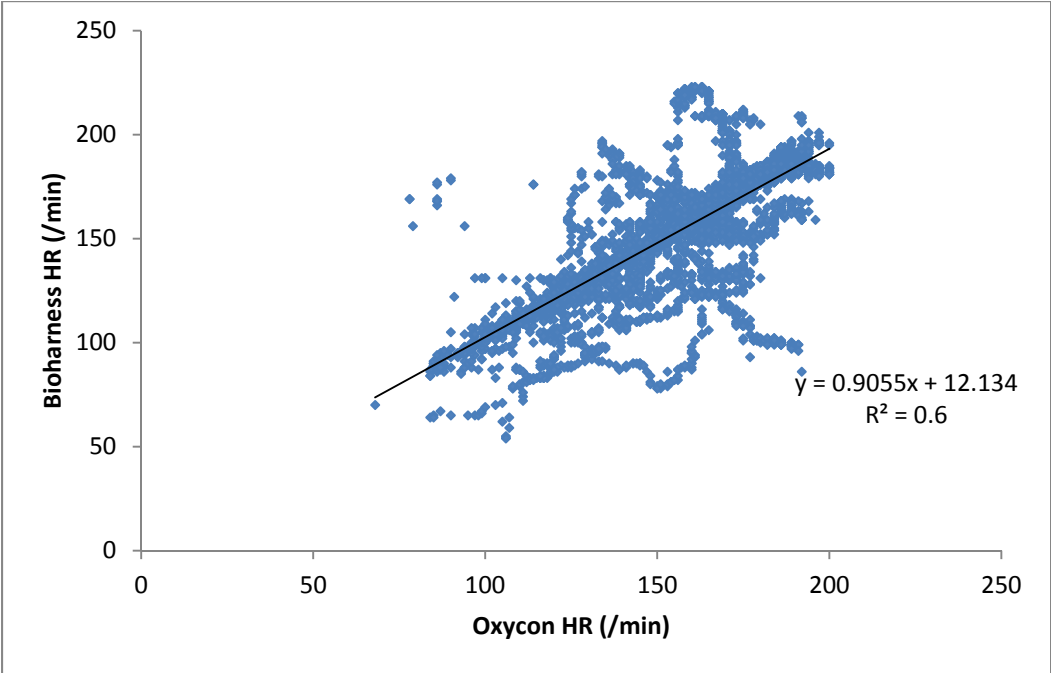


Figure 26. Bland-Altman for paired heart rates for all exercise data. Top and bottom horizontal lines signify ± 1.96 standard deviations.

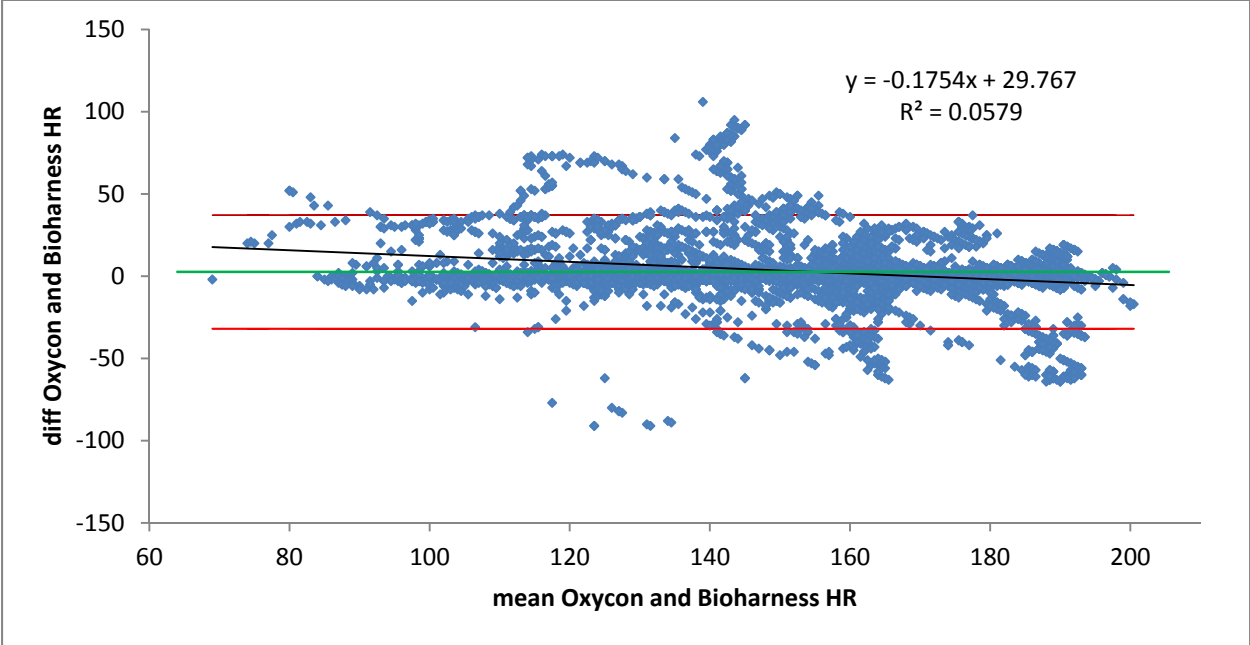


Figure 27. Paired breathing frequencies for all exercise data.

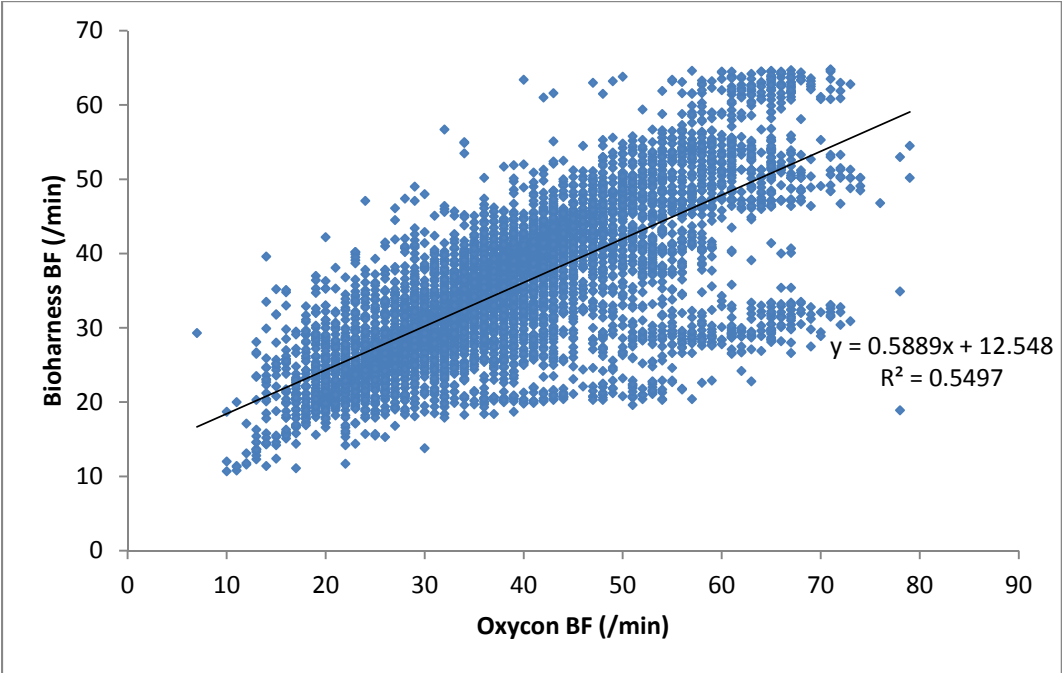


Figure 28. Bland-Altman for paired breathing frequencies for all exercise data. Top and bottom horizontal lines signify ± 1.96 standard deviations

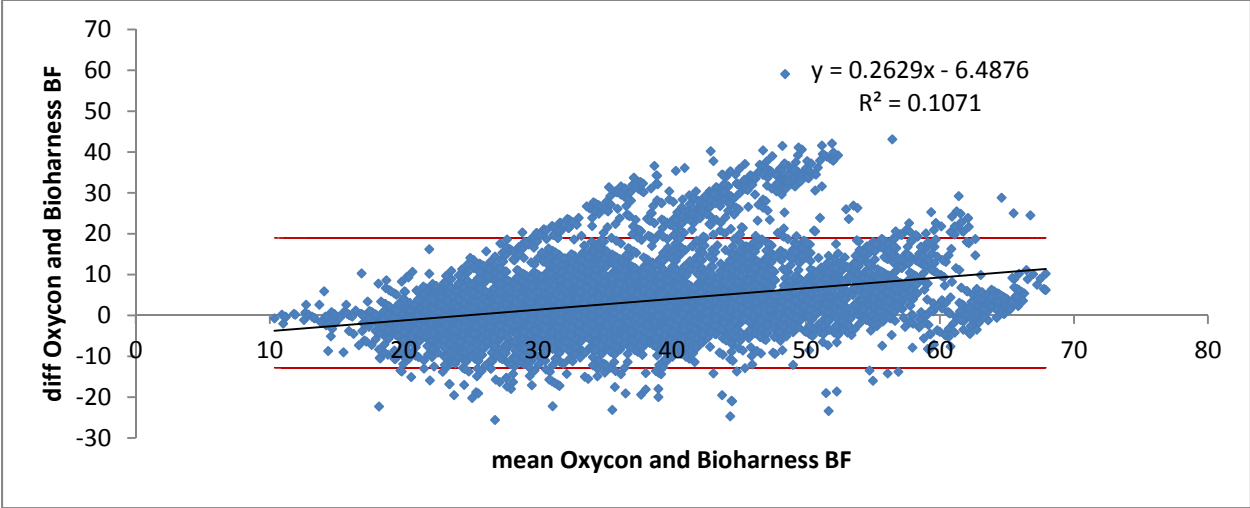


Figure 29. Linear increase in workrate over time for WFI Run protocol for each subject across 3 trials.

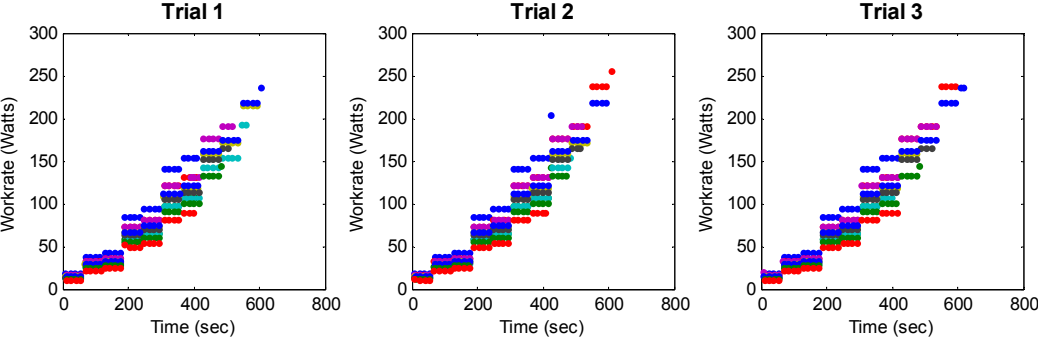


Figure 30. Linear increase in $\dot{V}O_2$ over workrate for each subject across 3 trials.

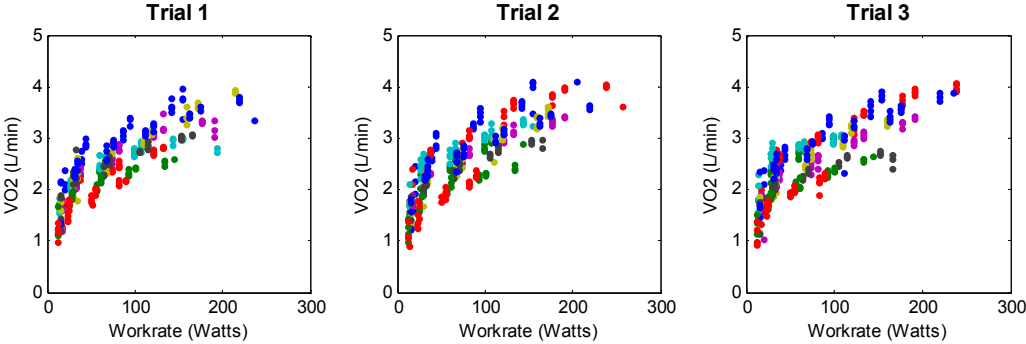


Figure 31. Linear increase in VMU over workrate for each subject across 3 trials.

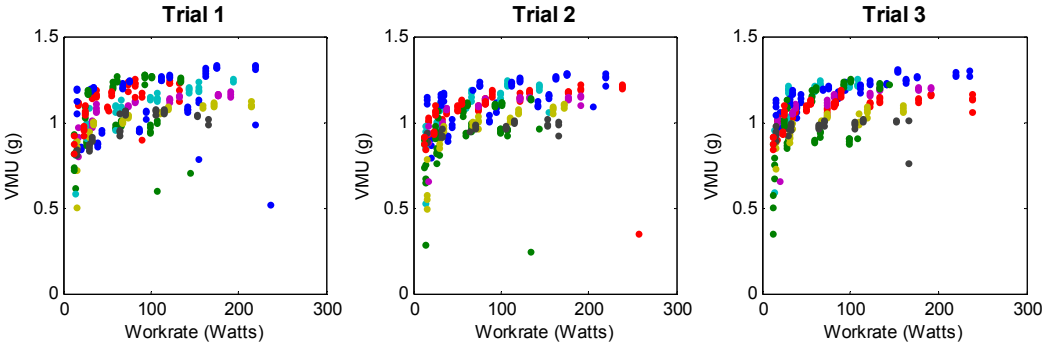


Figure 32. Linear increase in VMU against EE for each subject across 3 trials.

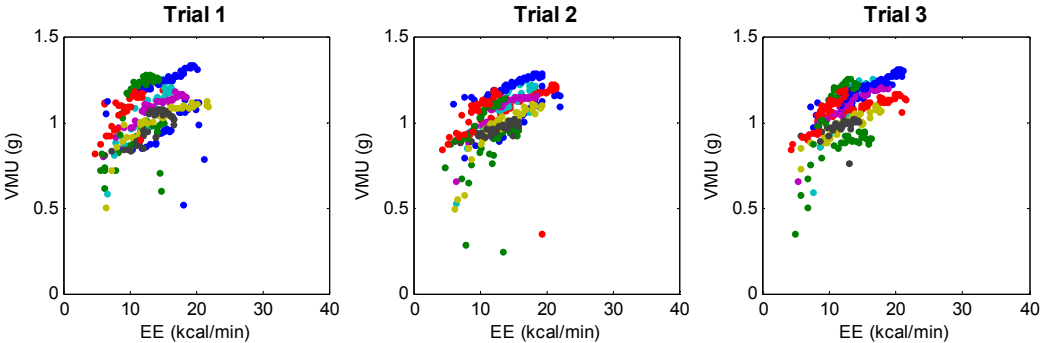


Figure 33. Linear increase in heart Rate against workrate for each subject across 3 trials.

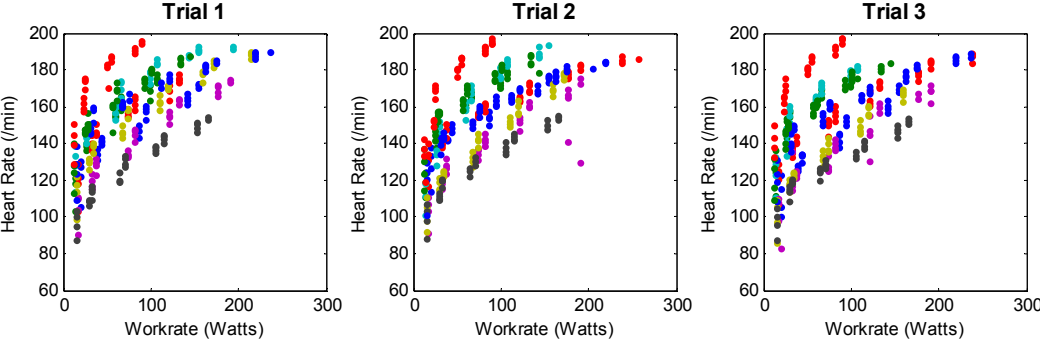


Figure 34. Chronotropic indices for each subject across 3 trials.

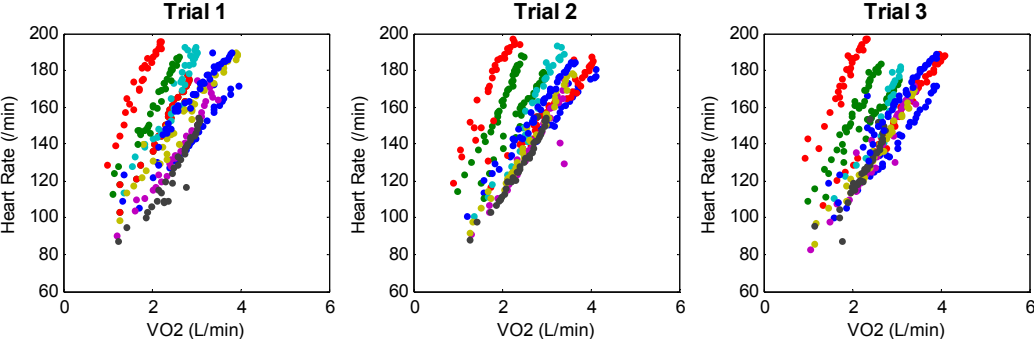


Figure 35. Stackplot with error bars for chronotropic indices.

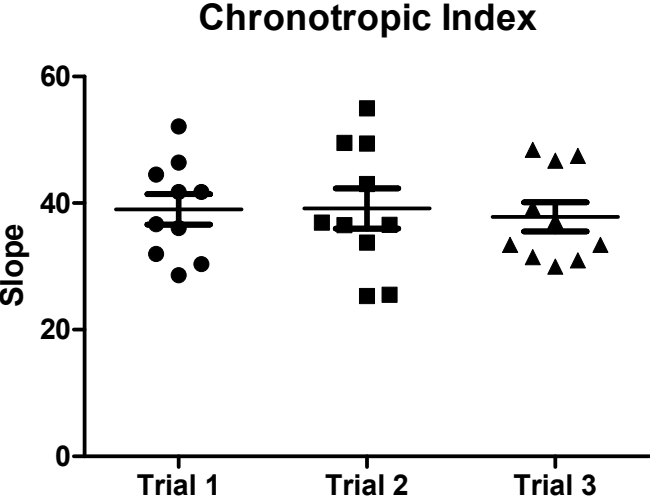


Figure 36. Cardiac indices for each subject across 3 trials.

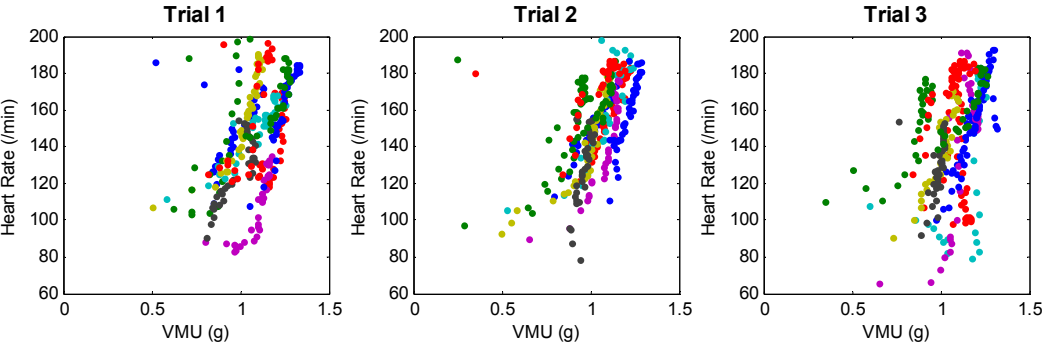


Figure 37. Stackplot with error bars for cardioaloric indices.

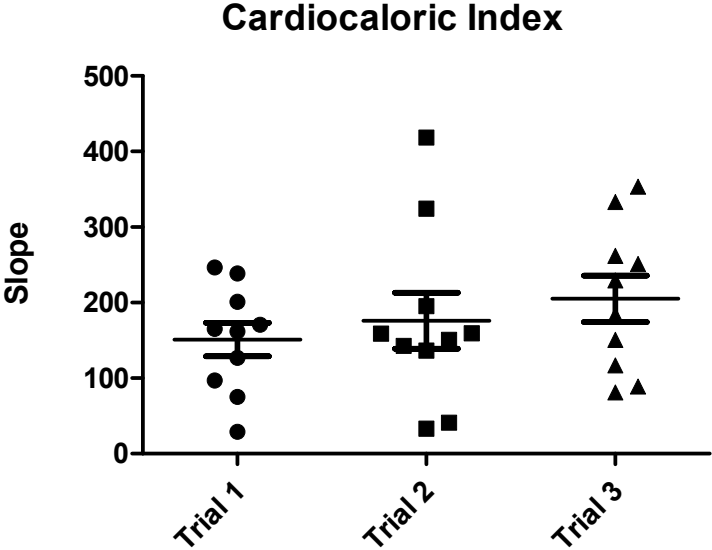
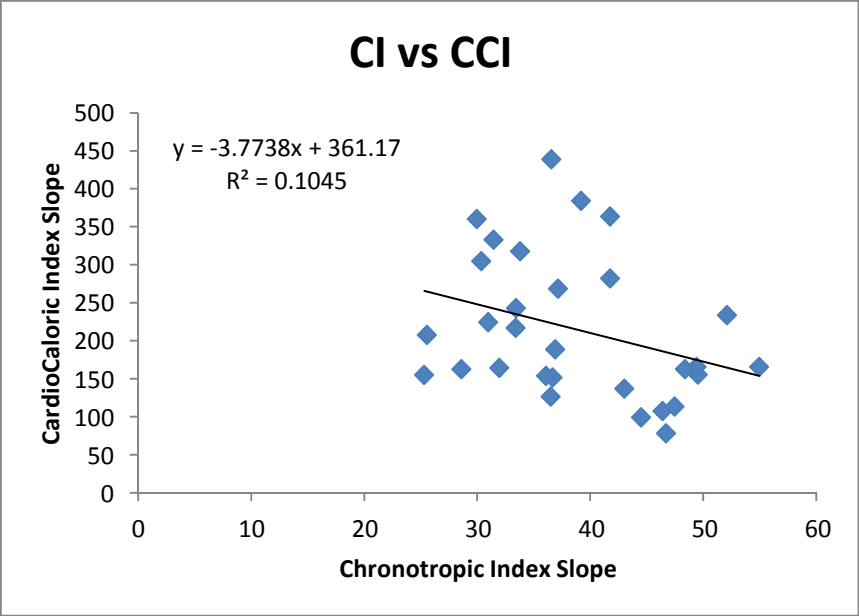


Figure 38. Linear regression for chronotropic index slope against cardioaloric index slope.



Appendix B: Tables

Table 1. Treadmill Matrix

		Speed (mph)		
		2.5	4	5.5
Grade (%)	0			
	2.5			
	5			

Table 2. Stepping Matrix

		Height (in)		
		6	10	20
Rate (bpm)	12			
	24			
	30			

Table 3. Subject Characteristics for Steady-State Exercise

	Age	Height	Weight	BMI
Men (n=8)	32 (10.7)	1.77 (0.1)	80.5 (11.6)	25.4 (3.0)
Women (n=2)	30 (8.4)	1.58 (0.1)	53.0 (2.2)	22.1 (0.3)
Total (n=10)	30.4 (9.9)	1.73 (0.2)	75.0 (15.5)	24.6 (3.1)

Values are mean (SD)

Table 4: Median Percentage of Variability (r^2) in Measured Energy Expenditure Explained by PAM

Treadmill	ΣA_{RL}	ΣA_{LL}	ΣA_{RA}	ΣA_{LA}	ΣA_{BL}	ΣA_{BA}	$\Sigma A_{BL,BA}$
<i>Median</i>	87%	86%	72%	86%	86%	81%	90%
<i>Mean</i>	84%	85%	70%	79%	85%	77%	87%

Table 5. Median Percentage of Variability (r^2) in Measured Energy Expenditure Explained by PAM

Stepping	ΣA_{RL}	ΣA_{LL}	ΣA_{RA}	ΣA_{LA}	ΣA_{BL}	ΣA_{BA}	$\Sigma A_{BL,BA}$
<i>Median</i>	73%	71%	36%	59%	72%	61%	73%
<i>Mean</i>	72%	68%	48%	52%	72%	57%	73%

Table 6. 2-factor ANOVA on PAM activity from Different Configurations for Treadmill Exercise

	Speed	Grade	Interaction
ΣA_{RL}	1.76 (p=0.07)	0.29 (p<0.001)	2.43 (p=0.06)
ΣA_{LL}	2.26 (p=0.05)	0.37 (p=0.001)	3.20 (p=0.09)
ΣA_{RA}	0.90 (p=0.26)	0.14 (p=0.003)	1.11 (p=0.16)
ΣA_{LA}	0.88 (p=0.30)	0.14 (p=0.004)	1.16 (p=0.21)
ΣA_{BL}	2.42 (p=0.05)	0.40 (p<0.001)	3.41 (p=0.06)
ΣA_{BA}	0.94 (p=0.28)	0.15 (p=0.006)	1.20 (p=0.19)
$\Sigma A_{BL,BA}$	1.73 (p=0.20)	0.29 (p=0.002)	2.33 (p=0.15)

Values reported in calculated F-like statistics (p-value).

Table 7. 2-factor ANOVA on PAM activity from Different Configurations for Stepping Exercise

	Step Height	Step Rate	Interaction
ΣA_{RL}	1.59 (p=0.15)	1.56 (p=0.05)	1.38 (p=0.15)
ΣA_{LL}	1.64 (p=0.31)	1.72 (p=0.27)	1.37 (p=0.19)
ΣA_{RA}	0.50 (p=0.43)	0.41 (p=0.31)	0.75 (p=0.32)
ΣA_{LA}	0.64 (p=0.39)	0.55 (p=0.22)	0.79 (p=0.27)
ΣA_{BL}	1.81 (p=0.16)	1.83 (p=0.10)	1.52 (p=0.13)
ΣA_{BA}	0.73 (p=0.37)	0.62 (p=0.19)	0.96 (p=0.28)
$\Sigma A_{BL,BA}$	1.59 (p=0.11)	1.44 (p=0.03)	1.54 (p=0.13)

Values reported in calculated F-like statistics (p-value).

Table 8: Subject Characteristics for Incremental Exercise

	Age	Height	Weight	BMI
Men (n=10)	30.1 (10.8)	1.73 (0.05)	74.7 (11.7)	25.0 (3.3)

Table 9. Speed and Grade Settings for WFI Run Protocol

Time		Speed	Grade
<i>Start</i>	<i>End</i>	<i>mph</i>	<i>%</i>
0:00	1:00	3.0	0
1:01	2:00	3.0	0
2:01	3:00	3.0	0
3:01	4:00	4.5	1
4:01	5:00	4.5	2
5:01	6:00	5.0	2
6:01	7:00	5.0	4
7:01	8:00	5.5	4
8:01	9:00	5.5	6
9:01	10:00	6.0	6
10:01	11:00	6.0	8
11:01	12:00	6.5	8
12:01	13:00	6.5	10
13:01	14:00	7.0	10
14:01	15:00	7.0	12
15:01	16:00	7.5	12
16:01	17:00	7.5	14
17:01	18:00	8.0	14

Table 10. Pearson R Correlations for HR Validity

Number of XY Pairs	8313
Pearson r	0.7746
95% confidence interval	0.7659 to 0.7831
P value (two-tailed)	P<0.0001
P value summary	***
Is the correlation significant? (alpha=0.05)	Yes
R squared	0.6000

Table 11. Single-factor ANOVA for Chronotropic Index Slopes Grouped by Trials

SUMMARY

<i>Groups</i>	<i>Count</i>	<i>Sum</i>	<i>Average</i>	<i>Variance</i>
Column 1	10	390.31	39.03	57.60
Column 2	10	391.66	39.17	100.33
Column 3	10	378.21	37.82	52.68

ANOVA

<i>Source of Variation</i>	<i>SS</i>	<i>df</i>	<i>MS</i>	<i>F</i>	<i>P-value</i>	<i>F crit</i>
Between Groups	11.0	2	5.5	0.08	0.93	3.35
Within Groups	1895.6	27	70.2			
Total	1906.5	29				

Table 12. Single-factor ANOVA for Chronotropic Index Slopes Grouped by Subjects

SUMMARY

<i>Groups</i>	<i>Count</i>	<i>Sum</i>	<i>Average</i>	<i>Variance</i>
Row 1	3	84.90	28.3	8.1
Row 2	3	118.24	39.4	27.2
Row 3	3	97.29	32.4	70.3
Row 4	3	141.53	47.2	6.4
Row 5	3	110.74	36.9	0.1
Row 6	3	101.90	34.0	5.4
Row 7	3	111.87	37.3	2.8
Row 8	3	95.65	31.9	3.1
Row 9	3	142.57	47.5	2.8
Row 10	3	155.50	51.8	10.9

ANOVA

<i>Source of Variation</i>	<i>SS</i>	<i>df</i>	<i>MS</i>	<i>F</i>	<i>P-value</i>
Between Groups	1632.7	9	181.4	13.25	0.000001
Within Groups	273.8	20	13.7		
Total	1906.5	29			

Table 13. Single-factor ANOVA for Cardiocaloric Index Slopes Grouped by Trials

SUMMARY

<i>Groups</i>	<i>Count</i>	<i>Sum</i>	<i>Average</i>	<i>Variance</i>
Trial 1	10	2020.4	202.0	7933.1
Trial 2	10	2055.1	205.5	9623.9
Trial 3	10	2381.4	238.1	10434.0

ANOVA

<i>Source of Variation</i>	<i>SS</i>	<i>df</i>	<i>MS</i>	<i>F</i>	<i>P-value</i>	<i>F crit</i>
Between Groups	7933.8	2	3966.90	0.43	0.66	3.35
Within Groups	251919.3	27	9330.35			
Total	259853.1	29				

Table 14. Single-factor ANOVA for Cardiacaloric Index Slopes Grouped by Subjects

SUMMARY

<i>Groups</i>	<i>Count</i>	<i>Sum</i>	<i>Average</i>	<i>Variance</i>
Row 1	3	541.1	180.4	1441.4
Row 2	3	742.6	247.5	12869.1
Row 3	3	849.3	283.1	5827.8
Row 4	3	366.8	122.3	855.0
Row 5	3	608.3	202.8	3578.0
Row 6	3	507.0	169.0	2075.8
Row 7	3	976.2	325.4	22901.9
Row 8	3	954.6	318.2	201.4
Row 9	3	350.2	116.7	1991.5
Row 10	3	560.8	186.9	1628.7

ANOVA

<i>Source of Variation</i>	<i>SS</i>	<i>df</i>	<i>MS</i>	<i>F</i>	<i>P-value</i>	<i>F crit</i>
Between Groups	153111.9	9	17012.4	3.19	0.01	2.39
Within Groups	106741.2	20	5337.1			
Total	259853.1	29				

Table 15: Statistical Parameter Summary for Incremental Treadmill Exercise

	ANOVA	CV	ICC
$\dot{V}O_2max$	0.85	6%	0.63
Endurance Time	0.91	6%	0.76
$\dot{V}O_2$ vs \dot{W}	0.94	6%	0.83
VMU vs \dot{W}	0.86	24%	0.66
VMU vs EE	0.97	24%	0.93
HR.bh vs \dot{W}	0.96	11%	0.90
HR.ox vs $\dot{V}O_2$	0.93	8%	0.80
HR.bh vs VMU	0.66	29%	0.31

References

1. Willbond SM, Laviolette MA, Duval K, Doucet E. Normal weight men and women overestimate exercise energy expenditure. *J Sports Med Phys Fitness*. 2010;50(4):377–384.
2. Sugimoto A, Hara Y, Findley TW, Yoncmoto K. A useful method for measuring daily physical activity by a three-direction monitor. *Scand J Rehabil Med*. 1997;29(1):37–42.
3. Welk GJ, Corbin CB, Kampert JB. The validity of the Tritrac-R3D activity monitor for the assessment of physical activity: II. Temporal relationships among objective assessments. *Res Q Exerc Sport*. 1998;69(4):395–399.
4. Tamura T, Fujimoto T, Sakaki H, Higashi Y, Yoshida T, Togawa T. A solid-state ambulatory physical activity monitor and its application to measuring daily activity of the elderly. *J Med Eng Technol*. 1997;21(3-4):96–105.
5. Heil DP, Bennett GG, Bond KS, Webster MD, Wolin KY. Influence of activity monitor location and bout duration on free-living physical activity. *Res Q Exerc Sport*. 2009;80(3):424–433.
6. Nichols JF, Patterson P, Early T. A validation of a physical activity monitor for young and older adults. *Can J Sport Sci*. 1992;17(4):299–303.
7. Curone D, Tognetti A, Secco EL, et al. Heart Rate and Accelerometer Data Fusion for Activity Assessment of Rescuers During Emergency Interventions. *IEEE Transactions on Information Technology in Biomedicine*. 2010;14(3):702 –710.
8. Crouter SE, Clowers KG. A novel method for using accelerometer data to predict energy expenditure. *J. Appl. Physiol*. 2006;100(4):1324–1331.
9. Howe CA, Staudenmayer JW, Freedson PS. Accelerometer prediction of energy expenditure: vector magnitude versus vertical axis. *Med Sci Sports Exerc*. 2009;41(12):2199–2206.
10. Jung JY, Han KA, Kwon HR, et al. The usefulness of an accelerometer for monitoring total energy expenditure and its clinical application for predicting body weight changes in type 2 diabetic korean women. *Korean Diabetes J*. 2010;34(6):374–383.
11. Reilly JJ, Kelly LA, Montgomery C, et al. Validation of Actigraph accelerometer estimates of total energy expenditure in young children. *Int J Pediatr Obes*. 2006;1(3):161–167.

12. Troiano RP. Translating accelerometer counts into energy expenditure: advancing the quest. *J. Appl. Physiol.* 2006;100(4):1107–1108.
13. Staudenmayer J, Pober D, Crouter S, Bassett D, Freedson P. An artificial neural network to estimate physical activity energy expenditure and identify physical activity type from an accelerometer. *J. Appl. Physiol.* 2009;107(4):1300–1307.
14. Crouter SE, Kuffel E, Haas JD, Frongillo EA, Bassett DR Jr. Refined two-regression model for the ActiGraph accelerometer. *Med Sci Sports Exerc.* 2010;42(5):1029–1037.
15. Crouter SE, Dellavalle DM, Haas JD, Frongillo EA, Bassett DR. Validity of ActiGraph 2-Regression Model and Matthews and NHANES and Cut-Points for Assessing Free-Living Physical Activity. *J Phys Act Health.* 2012. Available at: <http://www.ncbi.nlm.nih.gov/pubmed/22975460>. Accessed September 24, 2012.
16. Bouten CV, Westerterp KR, Verduin M, Janssen JD. Assessment of energy expenditure for physical activity using a triaxial accelerometer. *Med Sci Sports Exerc.* 1994;26(12):1516–1523.
17. Melanson EL Jr, Freedson PS. Validity of the Computer Science and Applications, Inc. (CSA) activity monitor. *Med Sci Sports Exerc.* 1995;27(6):934–940.
18. Plasqui G, Westerterp KR. Accelerometry and heart rate as a measure of physical fitness: cross-validation. *Med Sci Sports Exerc.* 2006;38(8):1510–1514.
19. Tönis TM, Gorter K, Vollenbroek-Hutten MMR, Hermens H. Comparing VO₂max determined by using the relation between heart rate and accelerometry with submaximal estimated VO₂max. *J Sports Med Phys Fitness.* 2012;52(4):337–343.
20. Cooper JA, Watras AC, O'Brien MJ, et al. Assessing validity and reliability of resting metabolic rate in six gas analysis systems. *J Am Diet Assoc.* 2009;109(1):128–132.
21. Zuntz N. Ueber die Bedeutung der verschiedenen Nährstoffe als Erzeuger der Muskelkraft. *Pflügers Archiv European Journal of Physiology.* 1901;83(10):557–571.
22. Rietjens GJ, Kuipers H, Kester AD, Keizer HA. Validation of a computerized metabolic measurement system (Oxycon-Pro) during low and high intensity exercise. *Int J Sports Med.* 2001;22(4):291–294.
23. Shrout PE, Fleiss JL. Intraclass correlations: uses in assessing rater reliability. *Psychol Bull.* 1979;86(2):420–428.

24. Weir JP. Quantifying Test-Retest Reliability Using the Intraclass Correlation Coefficient and the SEM. *The Journal of Strength and Conditioning Research*. 2005;19(1):231.
25. Herrmann SD, Barreira TV, Kang M, Ainsworth BE. Impact of accelerometer wear time on physical activity data: a NHANES semisimulation data approach. *Br J Sports Med*. 2012. Available at: <http://bjsm.bmj.com/content/early/2012/08/29/bjsports-2012-091410>. Accessed September 17, 2012.
26. Troiano RP, Berrigan D, Dodd KW, Mâsse LC, Tilert T, McDowell M. Physical activity in the United States measured by accelerometer. *Med Sci Sports Exerc*. 2008;40(1):181–188.
27. Thompson PD, Franklin BA, Balady GJ, et al. Exercise and Acute Cardiovascular Events Placing the Risks Into Perspective: A Scientific Statement From the American Heart Association Council on Nutrition, Physical Activity, and Metabolism and the Council on Clinical Cardiology. *Circulation*. 2007;115(17):2358–2368.